JOURNAL OF GEOPHYSICAL RESEARCH, VOL. 113, G02028, doi:10.1029/2007JG000635, 2008

Validation and intercomparison of global Leaf Area Index products derived from remote sensing data

S. Garrigues,[1] R. Lacaze,[2] F. Baret,[3] J. T. Morisette,[4] M. Weiss,[3] J. E. Nickeson,[5] R. Fernandes,[6] S. Plummer,[7] N. V. Shabanov,[8] R. B. Myneni,[8] Y. Knyazikhin,[8] and W. Yang[8]

Received 26 October 2007; revised 14 February 2008; accepted 20 March 2008; published 11 June 2008.

[1] This study investigates the performances of four major global Leaf Area Index (LAI) products at 1/11.2° spatial sampling and a monthly time step: ECOCLIMAP climatology, GLOBCARBON (from SPOT/VEGETATION and ATSR/AATSR), CYCLOPES (from SPOT/VEGETATION) and MODIS Collection 4 (main algorithm, from MODIS/TERRA). These products were intercompared during the 2001–2003 period over the BELMANIP network of sites. Their uncertainty was assessed by comparison with 56 LAI reference maps derived from ground measurements. CYCLOPES and MODIS depict realistic spatial variations at continental scale, while ECOCLIMAP poorly captures surface spatial heterogeneity, and GLOBCARBON tends to display erratic variations. ECOCLIMAP and GLOBCARBON show the highest frequency of successful retrievals while MODIS and CYCLOPES retrievals are frequently missing in winter over northern latitudes and over the equatorial belt. CYCLOPES and MODIS describe consistent temporal profiles over most vegetation types, while ECOCLIMAP does not show any interannual variations, and GLOBCARBON can exhibit temporal instability during the growing season over forests. The CYCLOPES, MODIS, and GLOBCARBON LAI values agree better over croplands and grasslands than over forests, where differences in vegetation structure representation between algorithms and surface reflectance uncertainties lead to substantial discrepancies between products. CYCLOPES does not reach high enough LAI values to properly characterize forests. In contrast, the other products have sufficient dynamic range of LAI to describe the global variability of LAI. Overall, CYCLOPES is the most similar product to the LAI reference maps. However, more accurate ground measurements and better representation of the global and seasonal variability of vegetation are required to refine this result.

Citation: Garrigues, S., et al. (2008), Validation and intercomparison of global Leaf Area Index products derived from remote sensing data, *J. Geophys. Res.*, *113*, G02028, doi:10.1029/2007JG000635.

1. Introduction

[2] Modeling Earth system processes requires observations of key surface characteristics provided at the relevant spatial and temporal resolution [*Cayrol et al.*, 2000]. Among these surface characteristics, the Leaf Area Index (LAI), defined as half the total developed area of green (i.e., photosynthetic active) leaves per unit ground horizontal surface area [*Chen and Black*, 1992], characterizes the structure and the functioning of vegetation. LAI is a key player in modeling ecosystem productivity [*Moulin et al.*, 1998; *Running et al.*, 1999; *Turner et al.*, 1999; *Zhang et al.*, 2005], and energy, mass (e.g., water, CO_2), and momentum exchanges between the surface and the atmosphere [*Dickinson*, 1995; *Sellers*, 1997; *Arora*, 2002; *Muñoz et al.*, 2008].

[3] Remote sensing observations acquired with moderate resolution optical sensors (with pixel sizes from 250 m to 7 km) allow monitoring the seasonal and interannual variability of LAI fields over regional to global domains [*Buermann et al.*, 2001; *Nemani et al.*, 2003; *Tian et al.*, 2004; *Zhang et al.*, 2004; *Gibelin et al.*, 2006; *Ahl et al.*, 2006]. Several LAI data sets have been produced from NOAA/AVHRR including that of *Sellers et al.* [1996] and *Los et al.* [2000]; that of Boston University [*Myneni et al.*, 1997; *Buermann et al.*, 2002; *Nemani et al.*, 2003] and ECOCLIMAP [*Masson et al.*, 2003]. More recently, three

[1] Earth System Science Interdisciplinary Center, University of Maryland, NASA Goddard Space Flight Center, Greenbelt, Maryland, USA.
[2] POSTEL Service Center/MEDIAS-France, Toulouse, France.
[3] INRA-EMMAH, UMR 1114, Avignon, France.
[4] NASA Goddard Space Flight Center, Greenbelt, Maryland, USA.
[5] INOVIM, NASA Goddard Space Flight Center, Greenbelt, Maryland, USA.
[6] Canada Centre for Remote Sensing, Ottawa, Ontario, Canada.
[7] IGBP-European Space Agency, Frascatti, Italy.
[8] Department of Geography and Environment, Boston University, Boston, Massachusetts, USA.

0148-0227/08/2007JG000635$09.00

global LAI products have been derived from SPOT/VEGETATION since 1998: CYCLOPES [*Baret et al.*, 2007], GLOBCARBON [*Deng et al.*, 2006], and one regional product produced by the Canada Centre for Remote Sensing (CCRS) over Canada [*Fernandes et al.*, 2003]. LAI products have been also generated from TERRA-AQUA/MODIS since 2000 [*Yang et al.*, 2006a]. Other global LAI data sets have been produced but either for a limited period of time including one from ADEOS/POLDER [*Roujean and Lacaze*, 2002; *Lacaze*, 2005] and one from ENVISAT/MERIS [*Bacour et al.*, 2006] or for a limited spatial coverage such as one from TERRA/MISR [*Knyazikhin et al.*, 1998; *Hu et al.*, 2003] and one from MSG/SEVIRI over Africa and Europe (http://landsaf.meteo.pt/).

[4] Assessing the uncertainties in LAI products through comparison with in situ measurements, i.e., direct validation, is critical for their proper use in land surface models [*Justice et al.*, 2000; *Morisette et al.*, 2006]. However, because direct validation is time and resource intensive, existing validation data sets are not representative of the global and seasonal variability of vegetation [*Baret et al.*, 2006]. Conversely, evaluating the temporal and spatial consistency between products, i.e., product intercomparison, can easily be achieved over a large number of sites representing the global distribution of land surface types and over a complete vegetation cycle. Product intercomparison provides additional information on the relative performance of each LAI retrieval algorithm - a key requirement to properly combine multiple LAI products and thus extend the temporal and spatial extents of LAI fields in land surface models.

[5] However, the validation and intercomparison of global LAI products is currently limited to few products [*Buermann et al.*, 2002; *Tian et al.*, 2004; *Abuelgasim et al.*, 2006; *Bacour et al.*, 2006; *Pisek and Chen*, 2007; *Weiss et al.*, 2007] and/or restricted spatiotemporal domains [*Chen et al.*, 2002; *Privette et al.*, 2002; *Cohen et al.*, 2006; *Morisette et al.*, 2006; *Yang et al.*, 2006b]. There is thus a need to provide the user community with a more comprehensive assessment of the uncertainties in existing global LAI products.

[6] The objective of this work is to validate and intercompare four global LAI products, namely: CYCLOPES (Carbon Cycle and Change in Land Observational Products from an Ensemble of Satellites), ECOCLIMAP, GLOBCARBON (GLOBal Biophysical Products Terrestial CARBON Studies), and MODIS (MODerate resolution Imaging Spectroradiometer), at 1/11.2° spatial sampling and a monthly time step. These products will be intercompared during the 2001–2003 period over the BELMANIP (Benchmark Land Multisite Analysis and Intercomparison of Products) network of sites, which represents the global variability of land surface types [*Baret et al.*, 2006]. The product uncertainties will be assessed using a large and unique validation data set, specially established for this exercise. The CCRS Canadian LAI product will be used as a regional reference to evaluate the performances of the considered global products over Canada. This work is a contribution to the global LAI validation and intercomparison initiative [*Morisette et al.*, 2006] established by the Land Product Validation (LPV, http://lpvs.gsfc.nasa.gov) subgroup of the Committee on Earth Observation Satellites (CEOS) Working Group on Calibration and Validation (WGCV).

[7] The second section of this paper provides a general background on the estimation of LAI from remote sensing observations. In the third section, the products investigated are described. The methodology for validating and intercomparing global LAI products is presented in section 4. Results are given in section 5 and discussed in section 6 with respect to user requirements and potential ways for improving global LAI products.

2. LAI Estimation From Remote Sensing Data

2.1. LAI Algorithm

[8] LAI estimation from remote sensing data is based on the analysis of multispectral and multidirectional surface reflectance signatures of photosynthetic vegetation elements. Two approaches are generally used to retrieve LAI from surface reflectances. The first one consists in establishing empirical or semi-empirical relationships between LAI and vegetation indices (i.e., combination of surface reflectances), designed to maximize sensitivity to the vegetation characteristics while minimizing confounding factors such atmospheric noise, soil background or view-illumination geometry [*Baret and Guyot*, 1991; *Myneni et al.*, 1995]. These relationships are specifically calibrated for distinct vegetation types using either concurrent in situ LAI and reflectance measurements [*Chen et al.*, 2002; *Fernandes et al.*, 2003] or simulations from canopy radiation models [*Myneni et al.*, 1997; *Deng et al.*, 2006]. The second approach is based on the inversion of a radiative transfer model [*Goel*, 1989; *Myneni et al.*, 1997; *Weiss and Baret*, 1999] simulating surface reflectances from canopy structural characteristics (including LAI), soil and leaf optical properties, and view-illumination geometry. Look Up Table (LUT) [*Knyazikhin et al.*, 1998] and neural network [*Weiss and Baret*, 1999; *Bacour et al.*, 2006] are the main inversion techniques used to retrieve LAI from radiative transfer models. The expected range of the model parameters is either set up for each vegetation type (e.g., MODIS algorithm) or globally (e.g., CYCLOPES algorithm).

[9] To remove residual atmospheric, cloud contamination and eventually view-illumination effects, pre- or post- processing steps can be applied to LAI retrieval. This includes compositing techniques, which consist in filtering reflectances (e.g., CYCLOPES algorithm) or LAI estimates (e.g., MODIS algorithm) within a given time window, and seasonal smoothing (e.g., GLOBCARBON, CCRS algorithms), which aims at identifying noisy data in the LAI seasonal trajectory and replace them by smoothed LAI values [*Sellers et al.*, 1996; *Chen et al.*, 2006a; *Gao et al.*, 2008].

2.2. Sources of Uncertainty in LAI Estimation

[10] Three major sources of uncertainties affect the estimation of LAI from surface reflectances. Because of the ill-posed nature of the inverse problem, the estimation of LAI from surface reflectances is unstable, i.e., small variations in surface reflectance can result in large variations in LAI estimate [*Knyazikhin et al.*, 1998; *Combal et al.*, 2002; *Tan et al.*, 2005]. Therefore, uncertainties in surface reflectance measurements, due to calibration errors, residual atmospheric and cloud contamination, background underneath the canopy (e.g., bright soil or snow cover), topography, view-illumination geometry effects (i.e., bidi-

rectional effects), and reflectance saturation in dense canopies, tend to destabilize the LAI estimation process [*Wang et al.*, 2001; *Fernandes et al.*, 2003; *Shabanov et al.*, 2005; *Yang et al.*, 2006a].

[11] The second source of uncertainty is related to the manner in which canopy architecture is represented in LAI retrieval algorithms. This mainly concerns the spatial variation of leaf area density leading to foliage clumping [*Nilson*, 1971; *Chen and Black*, 1992; *Weiss et al.*, 2004]. Not accounting for the foliage clumping in LAI retrieval algorithms leads to substantial underestimation of actual LAI, especially for needleleaf forest [*Chen et al.*, 1997]. Clumping occurs at several scales. At the plant scale, it corresponds to the spatial distribution of foliage elements along plant stems or trunks, branches, and shoots for trees. At the canopy scale, clumping depends on the spatial arrangement of plants within the canopy, as in the case of discontinuous canopies such as row crops. Finally, the clumping effect at the landscape scale is caused by the mosaic of vegetation patches such as forest stands, agricultural fields, or bare soils, which are often smaller than moderate resolution pixels [*Garrigues et al.*, 2006a]. Since most LAI retrieval algorithms are nonlinear and have been calibrated at the patch scale, their application over heterogeneous moderate resolution pixels can induce a scaling bias on LAI estimates that can reach up to 50% of the actual LAI value [*Chen*, 1999; *Tian et al.*, 2002; *Garrigues et al.*, 2006b]. Another source of uncertainty comes from the canopy vertical heterogeneity, in particular the presence of an understory layer that can substantially amplify the canopy LAI [*Chen et al.*, 1997; *Eriksson et al.*, 2006]. Canopy vertical heterogeneity is generally not properly taken into account in current global retrieval algorithms. In addition, while LAI is defined with reference to green foliage, non-green elements (e.g., senescent leaves) can contribute to the radiometric signal. However, this contribution is generally of second order because green leaves tend to cover non-green elements and the radiometric signal of non-green elements is generally close to that of bare soil. Nevertheless, since the impact of non-green surfaces in the canopy is generally not properly documented for the LAI products under study, some clarifications are needed, especially in the context of their utilization in land surface models.

[12] The last source of uncertainty concerns the applicability of the algorithm to a range of vegetation types and environmental conditions. LAI retrieval algorithms are based on inherent empirical assumptions on the distribution of their parameters that can depart significantly from actual canopy and soil characteristics. For example, classification errors in algorithms using a land cover map for their spatial extension can generate an LAI estimation error up to 50% of the actual value [*Myneni et al.*, 2002; *Fernandes et al.*, 2003]. Besides, the number of land cover classes can be too low to represent the global variability of vegetation structure.

3. Products Investigated

[13] We provide here the main characteristics of the products under study (see Table 1).

Table 1. Characteristics of the LAI Products Under Study[a]

Product Name	GSD	Temporal Sampling	Algorithm	Parameterization	Clumping Representation			Seasonal Smoothing	References
					Plant/Shoot Scale	Canopy Scale	Landscape Scale		
CYCLOPES-V3.1	1/112°	10 days	RTM 1D (neural network)	Global	No	No	Yes	No	*Baret et al.* [2007]
ECOCLIMAP	1/120°	1 month	Empirical (based on NDVI variations)	Vegetation type	Yes	Yes	No	No	*Masson et al.* [2003]
GLOBCARBON-V1	1/11.2°	1 month	Model derived VI-LAI relationship	Vegetation type	Yes	Yes	No	Yes	*Deng et al.* [2006]
MODIS-C4	1 km	8 days	*Main Alg*: RTM 3D (LUT) *Backup*: LAI-NDVI empirical relationship	Vegetation type	Yes	Yes	Yes	No	*Knyazikhin et al.* [1998] and *Yang et al.* [2006a]
CCRS	1 km	10 days	Empirical VI-LAI relationship	Vegetation type	Yes	Yes	Up to ~1 ha	Yes	*Fernandes et al.* [2003]

[a]All the products have global spatial coverage, except CCRS, which is restricted to Canada. VI, RTM, LUT, and GSD stands for "Vegetation Index", "Radiative Transfer Model", "Look Up Table" and "Ground Sampling Distance", respectively.

3.1. CYCLOPES

[14] The CYCLOPES LAI Version 3.1, distributed by http://postel.mediasfrance.org, is produced from the SPOT/VEGETATION sensor at 1/112° (about 1 km at equator) ground sampling distance (hereafter denoted GSD) and a 10-d temporal sampling, in a Plate Carrée projection, for the period 1999–2003 [*Baret et al.*, 2007]. Algorithm inputs are atmospherically corrected red, near-infrared (NIR), and shortwave-infrared (SWIR) reflectances normalized to a standard view-illumination geometry and with cloud or snow cover observations removed [*Hagolle et al.*, 2005]. The normalization is performed by inversion of a reflectance model [*Roujean and Lacaze*, 2002] over data acquired during a moving compositing period of 30 d displaced by 10-d shifts. CYCLOPES LAI is estimated using a neural network trained from one-dimensional radiative transfer model (SAIL model [*Verhoef*, 1984]) simulations. Estimations are weighted by an overall uncertainty of 0.04 on reflectances, accounting both for model and measurement uncertainties. Clumping at the plant and canopy scale is not represented in the CYCLOPES algorithm. Landscape clumping is partly taken into account by considering mixed pixels as a fraction of pure vegetation and pure bare soil when simulating the VEGETATION surface reflectance at the pixel level with the SAIL model. A flag value indicates when the retrieval algorithm fails, i.e., when there are less than two cloud- and snow-free observations in the compositing period (30 d) or when the retrieval is out of the valid range ([0–8]).

3.2. ECOCLIMAP

[15] The ECOCLIMAP database (http://www.cnrm.meteo.fr/gmme/PROJETS/ECOCLIMAP/page_ecoclimap.htm) provides a climatology of biophysical variables required for land surface modeling (including LAI), at 1/120° GSD and a monthly time step, in a Plate Carrée projection [*Masson et al.*, 2003]. The October 2004 version was used in this work. ECOCLIMAP is based on a global classification into 15 main surface classes derived from the combination of several land cover maps and a world climate distribution. For each class, the variation range of LAI is assigned from in situ measurements, which account for vegetation clumping at the plant and canopy scales and represent only green foliage including forest understory. Then, for each pixel of the ECOCLIMAP grid, global NOAA/AVHRR monthly composites of the Normalized Difference Vegetation Index (NDVI) covering an annual cycle (1997 for Europe and 1992–1993 for the rest of the world) are used to scale the temporal trajectory of LAI between the minimum and maximum LAI values of the corresponding pixel class. The premise for this approach is that LAI spatial variability within each vegetation class is low. In contrast to the other data sets under study, since ECOCLIMAP is a climatology, it does not describe interannual variations of LAI.

3.3. GLOBCARBON

[16] The GLOBCARBON LAI Version 1, distributed by http://geofront.vgt.vito.be/geosuccess/, is estimated for the period 1998–2003 from the combination of observations from two sensors: SPOT/VEGETATION and ENVISAT/AATSR (or the equivalent ATSR-2 for the 1998–2002 period for which ENVISAT/AATSR was not available). Individual estimates of LAI are produced for all the valid pixels from each sensor (atmospherically corrected, free from cloud, cloud shadow and snow) and then the median is computed at a 10-d time step from all the available values from all the sensors. The 10-d values are subjected to a smoothing and interpolation procedure [*Chen et al.*, 2006a]. The smoothed LAI observations are then averaged over a one month period and aggregated to 1/11.2° GSD (about 10 km at equator) in a Plate Carrée projection. The GLOBCARBON algorithm [*Deng et al.*, 2006] relies on land cover-specific relationships between LAI and combinations of red, NIR, and SWIR spectral bands, which were derived using the Four Scale canopy reflectance model [*Chen and Leblanc*, 2001]. The algorithm also accounts for vegetation clumping at the plant and canopy scales by application of a cover-type dependent clumping index defined by *Chen et al.* [2005]. The global application of the algorithm is achieved using the Global Land Cover 2000 (GLC2000) map [*Bartholome and Belward*, 2005]. A flag value indicates when no LAI estimate is computed, i.e., when there are no clear observations and for particular GLC2000 classes (burnt and bare area, snow and ice area, artificial surfaces).

3.4. MODIS

[17] The TERRA MODIS LAI Collection 4, available from http://edcimswww.cr.usgs.gov/pub/imswelcome/, is considered here. Note that the upcoming MODIS LAI collection 5 [*Yang et al.*, 2006c] was not available at the start of this work and our results are restricted to Collection 4. The Collection 4 data set was produced between February 2000 through 2006 at 1 km GSD and a 8-d time step over a sinusoidal grid [*Yang et al.*, 2006a, 2006b]. The main algorithm is based on LUTs simulated from a three-dimensional radiative transfer model [*Knyazikhin et al.*, 1998]. The MODIS red and NIR atmospherically corrected reflectances [*Vermote et al.*, 1997] and the corresponding illumination-view geometry are used as inputs of the LUTs. The algorithm output is the mean LAI computed over the set of acceptable LUT elements for which simulated and measured MODIS surface reflectances differ within specified levels of model and surface reflectance uncertainties. When the main algorithm fails, a backup algorithm based on LAI-NDVI relationships, which were calibrated over the same simulations used to build the LUTs of the main algorithm, is used to estimate LAI. The backup algorithm provides an LAI of lower accuracy when compared to main algorithm retrievals [*Yang et al.*, 2006a]. MODIS LAI retrievals are executed irrespective of cloud and snow state but the majority of retrievals under these conditions or under residual atmospheric contamination are performed by the back-up algorithm [*Yang et al.*, 2006a]. Parameters of both main and backup algorithms are defined for 6 vegetation types and the MODIS land cover map [*Friedl et al.*, 2002] is used for the global application of both algorithms. The MODIS algorithm accounts for vegetation clumping at the canopy and plant (shoot) scales through 3D radiative transfer formulations. The clumping at the landscape scale is partly addressed via mechanisms based on the radiative transfer theory of canopy spectral invariants [*Knyazikhin et al.*, 1998; *Tian et al.*, 2002; *Huang*

et al., 2007]. LAI is first produced daily, and then the LAI value generated from the main algorithm (if none available, back-up retrievals) and corresponding to the maximum Fraction of Photosynthetically Active Radiation (fPAR) absorbed by the canopy (a variable also retrieved by the MODIS algorithm) is selected over an eight-day period. In this work, only main algorithm retrievals are considered as valid data. Note that no LAI is retrieved over bare and very sparsely vegetated areas, perennial ice and snow areas, permanent wetlands, urban, and water bodies.

3.5. CCRS

[18] The CCRS LAI product has been produced from SPOT/VEGETATION surface reflectances, normalized to a common acquisition geometry, at 1 km GSD and a 10-d time step over Canada, since 1998 until present, in a Lambert conical projection [*Fernandes et al.*, 2003]. The algorithm relies on empirical relationships between in situ LAI measurements and vegetation indices for seven cover classes corresponding to vegetated surfaces types in Canada. Clumping is explicitly included up to scales of ~1 ha through calibration of vegetation indices to field data sets. For forested areas, understory above a datum of 1.35 m (breast height) is included. The application of the algorithm to Canada is achieved using a regional land cover map derived from SPOT/VEGETATION data [*Cihlar et al.*, 2003]. Over mixed (evergreen needleleaf and deciduous broadleaf) forest pixels, a needleleaf cover fraction (derived from SPOT/VEGETATION and ancillary data) is used to linearly weight the relationships related to each pure forest class. The output LAI estimates are smoothed over a moving window of ~30 d. This product is used here as a regional reference data set as it has been extensively validated against field data [*Chen et al.*, 2002; *Fernandes et al.*, 2003; *Abuelgasim et al.*, 2006] and generally meets CEOS performance targets during snow free periods.

4. Methodology

4.1. Intercomparison Approach

4.1.1. Global Network of Sites

[19] The LAI products were intercompared over the BELMANIP network of sites that was designed to represent the global variability of land surface types [*Baret et al.*, 2006]. This benchmark network brings together 404 sites (full list at http://lpvs.gsfc.nasa.gov/lai_intercomp.php) extracted from several existing networks (AERONET, FLUXNET, VALERI, EOS Land Validation Core Sites, BigFoot, etc.). The land surface type of each BELMANIP site is defined using seven generic classes derived from the ECOCLIMAP classification (*Masson et al.*, 2003). In this paper, the LAI products are analyzed for the 5 generic vegetation classes from ECOCLIMAP, namely: grass, crop, evergreen needleleaf forest (ENF), deciduous broadleaf forest (DBF), evergreen broadleaf forest (EBF).

4.1.2. Resampling LAI Products to Common Spatial and Temporal Supports

[20] The LAI products must be compared over a similar spatial support area and temporal support period. They were thus resampled over the GLOBCARBON grid at 1/11.2° GSD and at a monthly time step, which are the coarsest spatial and temporal supports of the products investigated. This approach is in agreement with other studies [*Chen et al.*, 2002; *Fernandes et al.*, 2003; *Tan et al.*, 2006; *Weiss et al.*, 2007; *Tarnavsky et al.*, 2008] that suggest comparing remote sensing products at a substantially larger GSD than their native GSD to reduce potential coregistration errors between products and differences in sensor Point Spread Function (i.e., the PSF that determines the actual footprint of the data). The LAI for each 1/11.2° target pixel was computed as the average of the reprojected native pixels of a given product with pixel centers falling within the 1/11.2° area and the one month temporal window. A no-data value was assigned if more than half of the native pixels falling within the 1/11.2° area and the one-month temporal window are composed of invalid data.

4.2. Direct Validation Approach

4.2.1. LAI Reference Maps

[21] An important issue related to the validation of moderate resolution products is the support area mismatch between ground LAI measurement and moderate resolution pixel. The "state of the art" direct validation approach [*Morisette et al.*, 2006] consists in using high spatial resolution imagery (with GSD between 20 m and 30 m) to scale the ground LAI measurements up to moderate resolution pixel. For this, a "transfer function" between high spatial resolution surface reflectances and LAI measurements is established, and then is applied to an appropriate extent of the high spatial resolution image. The resulting high spatial resolution LAI map is finally aggregated to larger pixel size for comparison with moderate resolution products.

[22] A total of 81 LAI reference maps (Table 2) were compiled over a subset of 41 of the BELMANIP sites between 2000 and 2004 through a coordinated international effort of the CEOS-WGCV LPV Sub-Group [*Morisette et al.*, 2006]. The validation sites are selected to be homogeneous in terms of land cover type, vegetation composition and topography. The typical surface of the validation sites is between 9 km^2 and 100 km^2, except for the CCRS sites corresponding to larger study areas of Canada (up to 54000 km^2). These large CCRS sites were cropped into multiple spatial subsets (Table 2) and each subset was used as an independent validation map.

4.2.2. Uncertainties in LAI Reference Maps

[23] LAI reference map accuracy is primarily affected by ground measurement errors [*Fernandes et al.*, 2003]. The most accurate measurement is achieved using destructive samplings for foliage element area estimates, and locally calibrated allometric relationships to scale these estimates over plots [*Chen et al.*, 1997; *Jonckheere et al.*, 2004]. Because destructive techniques are too laborious to sample LAI over large areas, optical indirect techniques based on the analysis of light transmittance through the canopy [*Chen et al.*, 1997; *Jonckheere et al.*, 2004] are generally used to measure LAI. Optical measurements provide an effective LAI associated with several sources of uncertainties [*Chen et al.*, 1997; *Gower et al.*, 1999; *Weiss et al.*, 2004; *Chen et al.*, 2006b]. First, they do not generally take into account foliage clumping, resulting in an underestimation of LAI up to 70% over coniferous forests [*Chen and Cihlar*, 1995; *Stenberg*, 1996]. Second, optical measurements usually do not distinguish between photosynthetically active tissues

Table 2. Characteristics of the Validation Sites (Total 41) and Associated LAI Reference Maps Under Study (Total 81)[a]

Site	Location	Lat	Lon	LC	Dates	Mean LAI	Clu.	Un.	GL	Ref
Chequamegon	USA	45.95	−90.27	MF	2002/8/1	3.4	0	0	0	1
Harvard	USA	42.53	−72.17	MF	2001/7/26; 2002/8/24	[4.6 4.7] 4.7	0	0	0	
Konza	USA	39.09	−96.57	Grass	2001/8/16; 2001/6/18	[2.6 2.9] 2.8	1	Na	1	
Metolius	USA	44.45	−121.57	ENF	2002/9/24	2.5	0	0	0	
NOBS (Boreas)	Canada	55.89	−98.48	ENF	2001/7/14; 2002/7/14	[2.7 3] 2.9	1	0	0	
Sevilleta	USA	34.35	−106.69	Grass	2002:7/26, 8/22, 9/09, 11/15 2003:6/23, 7/28, 9/15, 11/21	[0.05 0.4] 0.2	1	Na	1	
Tapajós	Brazil	−2.87	−54.95	EBF	2002/2/15	6.1	0	0	0	
Tundra	USA	71.27	−156.61	Grass	2002/8/15	1.1	1	Na	1	
Alpilles01	France	43.81	4.75	Crop	2001/3/15	1	0	0	0	2
Flakaliden	Sweden	64.11	19.47	ENF	2002/8/20	2.3	0	0	0	
Ruokolahti	Finland	61.53	28.71	ENF	2000/6/10	1.7	1	0	1	
Chateauguay (×4)	Canada	44.91	−74.36	MF	2001/6/15	[2.1 4.1] 3.1	1	0	1	3
Larose	Canada	45.38	−75.17	MF	2003/8/19	3.2	1	1	1	
SW-Ontario (×15)	Canada	45.29	−78.60	MF	2002/8/15	[2.8 4] 3.4	1	0	1	
Thompson (×4)	Canada	56.05	−98.16	ENF	2001/7/15	[1.4 2] 1.7	1	0	1	
Kejimikujik (×2)	Canada	44.45	−65.28	MF	2000/7/15	[2.9 3.3] 3.1	1	0	1	
Watson Lake (×3)	Canada	60.10	−129.69	MF	2000/7/15	[2 2.4] 2.2	1	0	1	
Appomattox	USA	37.22	−78.88	MF	2002/8/5	1.9	1	1	1	4
Walnut Creek	USA	41.96	−111.61	Crop	2002/6/23; 2002/7/08	[1.4 2.8] 2.1	0	0	0	5
Chamela (×2)	Mexico	19.71	−105.01	MF	2001/8/15	[4.5 4.6] 4.55	0	0	0	6
Los Inocentes	Costa Rica	11.03	−85.50	EBF	2000/6/15	2.5	0	0	0	
AekLoba	Sumatra	2.63	99.58	EBF	2001/6/1	3.5	0	1	0	7
Alpilles02	France	43.81	4.71	Crop	2002/7/20	1.7	1	1	0	
Barrax	Spain	39.07	−2.10	Crop	2003/7/3	1	0	1	0	
Concepción	Chile	37.47	−73.47	ENF	2003/1/23	3.1	0	1	0	
Counami	French Guyana	5.34	−53.24	EBF	2002/10/1; 2001/09/26	[4.4 4.9] 4.7	1	1	0	
Fundulea	Romania	44.41	26.58	Crop	2001/3/17; 2002/6/9; 2003/5/31	[1.1 1.5]	0; 1; 0	1	0	
Gilching	Germany	48.08	11.32	Crop	2002/7/8	5.4	1	1	0	
Gourma	Mali	15.32	−1.56	Grass	2001/10/1	1.2	0	Na	0	
Haouz	Morocco	31.66	−7.60	Crop	2003/3/25	1.2	0	1	0	
Hirsikangas	Finland	62.64	27.01	ENF	2003/8/2	2.5	0	0	0	
Jarvselja	Estonia	58.30	27.26	MF	2002/7/13; 2003/6/26	4.2	0	1	0	
Laprida	Argentina	36.99	−60.55	Grass	2002/11/13	2.8	1	Na	0	
Larzac	France	43.94	3.12	Grass	2002/7/12	0.8	1	Na	0	
Rovaniemi	Finland	66.46	25.35	ENF	2004/7/23	1.3	0	1	0	
Sud-Ouest	France	43.51	1.24	Crop	2002/7/20	2	1	1	0	
Turco	Bolivia	18.24	−68.19	Grass	2002/8/29; 2003/4/25	[0.04 0.07] 0.05	1;0	Na	0	
Sonian	Belgium	50.77	4.41	MF	2004/7/28	5.6	1	1	0	
Nezer	France	44.57	−1.05	ENF	2002/4/21	2.1	1	1	0	
Camerons	Australia	32.60	116.25	EBF	2004/4/6	2.1	1	1	0	
Puechabon	France	43.72	3.65	MF	2001/06/12	2.8	1	1	0	

[a]"Lat", "Lon", "LC", "Clu", "Un", "GL", and "Ref" stand for "latitude", "longitude", "land cover", "clumping", "understory", "green LAI" and "reference", respectively. In the column "Site" the number in parenthesis indicates multiple spatial subsets over the site. In the column "LC", ENF, EBF and MF stand for evergreen needleleaf forest, evergreen broadleaf forest and mixed (evergreen needleleaf + deciduous broadleaf) forest, respectively. When multiple spatial or temporal subsets are available over the same site, the column "Mean LAI" provides the variation range of LAI (number into brackets) followed by the mean value. In the columns "Clu" and "Un", the value 1 (0) means that clumping and understory have (have not) been taken into account in the LAI measurement. In the column "GL", the value 1 indicates that only green elements are quantified excluding woody and senescent materials while 0 indicates that total Plant Area Index is measured. The column "Ref" indicates the research group and associated references for each validation site. The numbers refer to 1: BigFoot [*Cohen et al.*, 2006], 2: Boston University [*Yang et al.*, 2006b], 3: CCRS [*Abuelgasim et al.*, 2006], 4: U.S. Environmental Protection Agency [*Iiames et al.*, 2004], 5: SMEX02 [*Anderson et al.*, 2004], 6: University of Alberta [*Kalacska et al.*, 2004, 2005a, 2005b], and 7: VALERI [*Baret et al.*, 2008]. More information on each site and full list of validation sites can be found on the LPV website (http://lpvs.gsfc.nasa.gov).

and other plant elements such as branches, stems, trunks, and senescent leaves, leading to a positive bias in measured LAI [*Kucharik et al.*, 1998; *Barclay et al.*, 2000; *Stenberg et al.*, 2003; *Chen et al.*, 2006b]. Third, forest understory is not systematically taken into account in ground LAI measurements. This can result in substantial differences with the satellite LAI product derived from the vertical integration of the radiometric signal within the canopy [*Chen et al.*, 1997; *Iiames et al.*, 2004; *Wang et al.*, 2004; *Abuelgasim et al.*, 2006]. Other sources of measurement error include saturation of optical signal in dense canopies [*Aragao et al.*, 2005], simplification of leaf optical properties [*Leblanc and Chen*, 2001] and insufficient spatial sampling within a plot [*Weiss et al.*, 2004; *Garrigues et al.*, 2008b]. For a subset of the LAI maps used in this work, some of these measurement errors have been corrected using appropriate techniques (Table 2). Note, also, that contrary to moderate resolution LAI products, high spatial resolution LAI reference maps

are not affected by landscape clumping and can be considered free from scaling errors when aggregated to larger pixel size [*Garrigues et al.*, 2006b].

[24] While the overall uncertainty of each LAI reference map has not been documented, the typical LAI reference map corrected for clumping and non-green elements is reasonably expected to be within ±20% relative uncertainty or within an absolute uncertainty smaller than 1 LAI for most sites [*Fernandes et al.*, 2003]. When the high spatial resolution LAI reference map is aggregated to a ~10 km pixel size, most spatially random errors cancel out, decreasing the overall uncertainty by 50% and leaving only the measurement bias [*Fernandes et al.*, 2001; *Butson and Fernandes*, 2004]. For effective LAI maps, the remaining bias is larger, due to the impact of clumping and non-green vegetation. Since the main source of uncertainty is the foliage clumping, only the LAI maps corrected for clumping (56 of the 81 LAI reference maps) will be used for the direct validation.

4.2.3. Comparison With Moderate Resolution LAI Products

[25] For all the products under study, the LAI value from the 1/11.2° target pixel containing the center of the validation site and from the month including the date of the ground measurement is extracted and compared with the LAI reference map aggregated within the 1/11.2° pixel. For the sites having a surface smaller than that of the 1/11.2° pixel, the mean LAI reference map value over the site is extracted. Since most of these sites are homogeneous over areas larger than their actual size [*Baret et al.*, 2008], the surface mismatch between the 1/11.2° pixel and the smaller LAI reference map only slightly affects validation results. The temporal mismatch between the monthly LAI value of the global product and the single date ground measurement should not impact validation results over evergreen forest sites, for which LAI is reasonably stable over one month. However, it can be a source of uncertainty over highly dynamic targets such as croplands, grasslands, and deciduous forests. For few forest sites, for which no validation data was available for the period under study (2001–2003), and for which interannual LAI variations are low over this period, we compared measurements collected in 2000 (2004) with the value of the global product acquired in 2001 (2003) for the same month. This choice was made since we were able to verify that no disturbances (e.g., fires, deforestation, etc.) occurred from 2000 (2003) to 2001 (2004) for these sites. Generally, scatter due to possible spatial and temporal mismatches between the LAI reference map and the moderate resolution product is minor compared to overall uncertainties of the LAI reference maps, and will not be explicitly considered here.

5. Results

[26] Discrepancies between the LAI products (or between the LAI products and the LAI reference maps) are quantified by the following metrics: the r^2, the *RMSE*, the bias (denoted *B*) and the standard deviation of the difference between LAI products, i.e., the random fluctuation between products (denoted *S*). Note that B and S are two subcomponents of the total discrepancy quantified by the RMSE ($RMSE^2 = B^2 + S^2$).

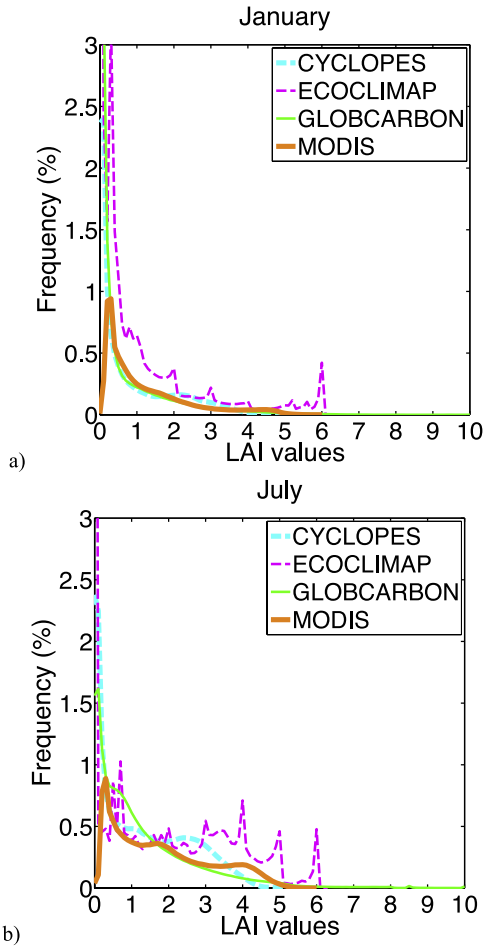

Figure 1. Global LAI value distribution for each product under study for (a) January and (b) July over the 2001–2003 period. Frequency is given in percentage of total number of pixel of the global grid. For clarity of presentation, the range of frequency (*y* axis) has been limited to 3%. The actual frequency of null LAI value for ECOCLIMAP is 12.95% for January and 12.79% for July. The actual frequency of null LAI for GLOBCARBON in January is 7.8%. Note, also, that few GLOBCARBON values are larger than 10, not represented here for clarity.

5.1. Intercomparison

5.1.1. Spatial Consistency

5.1.1.1. Global Distribution

[27] Figure 1 displays the distribution of LAI values for each product computed over their global grid for two particular months (January and July) during the 2001–2003 period. CYCLOPES, MODIS, and GLOBCARBON show continuous and smooth LAI distribution as expected at global scale. Conversely, ECOCLIMAP displays erratic distributions with local maxima at integer values of LAI. This is highly unrealistic and reflects the empirical nature of this product. For all the products, the frequency of low (high) LAI values decreases (increases) between January and July in agreement with the growing season over northern latitudes. Differences between product global distributions are smaller in January than in July, suggesting that most discrepancies between products occur during the

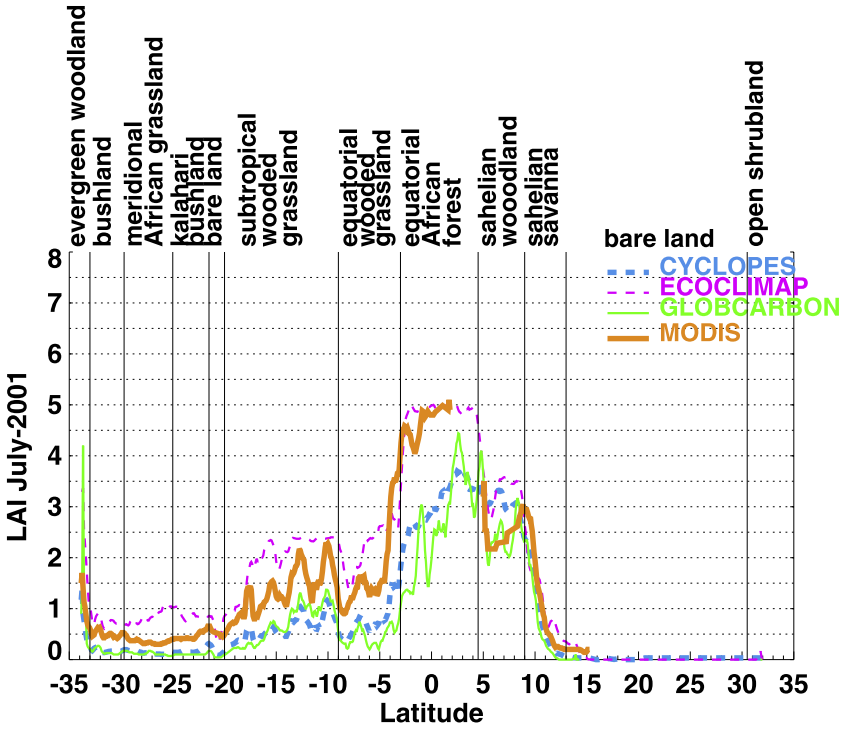

Figure 2. Transect of GLOBCARBON, CYCLOPES, ECOCLIMAP, and MODIS LAI products over Africa (along 25° east) for July 2001. The land cover classes are extracted from the ECOCLIMAP classification [*Masson et al.*, 2003].

growing season over northern latitudes. The higher frequencies shown by ECOCLIMAP compared to the other products are explained by the lack of missing data in its algorithm (see section 5.1.2). In particular, ECOCLIMAP shows much higher frequency of null LAI values compared to CYCLOPES, GLOBCARBON, and MODIS. Indeed, for these latter products the permanent ice areas are encoded as missing data while null LAI values are assigned in ECOCLIMAP. The frequency of low LAI values is much smaller for MODIS than for the other products, particularly in January. This is partly due to the overestimation of MODIS LAI over sparse vegetation and during the dormant season over DBF (see section 5.1.2). MODIS also has few null LAI values because bare and very sparsely vegetated lands, perennial ice and snow areas, permanent wetlands, urban, and water bodies are all masked in the MODIS algorithm. CYCLOPES rarely reaches LAI values larger than 4, indicating substantial underestimation over dense forests. In contrast, other products have a sufficient dynamic range of LAI to describe the global variability of LAI. The highest LAI values reached by GLOBCARBON, exceeding 10, are potentially unrealistic for 1/11.2° areas and are probably caused by artifacts from the smoothing process.

5.1.1.2. Regional Consistency

[28] The spatial consistency between products is now conducted at the regional scale. While all the continents have been analyzed, we present here the results over Africa and Canada, which illustrate the main spatial inconsistencies between products.

[29] Figure 2 displays CYCLOPES, ECOCLIMAP, GLOBCARBON and MODIS LAI values extracted along a 25° east longitude transect over Africa for July 2001.

[30] The best spatial continuity (i.e., no data gaps) along this transect is achieved for ECOCLIMAP, given it is a climatology, and GLOBCARBON, which benefits from multisensor observations and includes a gap filling processing in its algorithm. However, the GLOBCARBON spatial trajectory is highly noisy, particularly over the equatorial forest, which is possibly due to residual cloud or atmospheric effects. Since the ECOCLIMAP approach assumes low spatial variability within each vegetation class (see section 3.2), it is limited to capture the surface spatial heterogeneity within each vegetation class as compared to the other satellite products (e.g., wooded grassland, Figure 2). Two groups of product can be distinguished from this figure. First, CYCLOPES and GLOBCARBON derived from the same SPOT/VEGETATION observations describe very similar spatial variations and LAI magnitude over grassland and bushland. Second, MODIS and ECOCLIMAP show good agreement over equatorial forest, where they provide more realistic high LAI values compared to the low values from CYCLOPES and the very noisy values from GLOBCARBON.

[31] The global products are now compared to the CCRS LAI map over Canada considered here as a regional reference (see section 3.5). Figure 3 displays the differences between each global LAI map and the CCRS LAI map for July 2003.

[32] Overall, the CCRS map captures more spatial details than the other global products. This is mainly due to the finer land cover map used in the CCRS algorithm, which includes distinct types of crops, a representation of mixed needleleaf and broadleaf forest, and an accurate mapping of water bodies at the subpixel scale. For example, the visual

comparison of the global product maps to the CCRS map in the south provinces of Canada (figures not shown here for brevity) indicates that all the global products are quite homogeneous over this region while the CCRS map resolves small vegetation patches (see the red box on Figure 3). All the global products (except ECOCLIMAP) underestimate LAI over these patches since they consist of mixed crop areas (corn, sorghum, canola [cf. *Latifovic et al.*, 2004]) that are not properly described in the global algorithms. Conversely, the area within the green box is mainly composed of grassland and cereal crops [*Latifovic et al.*, 2004], over which all the global products (except ECOCLIMAP) agree with the CCRS LAI map.

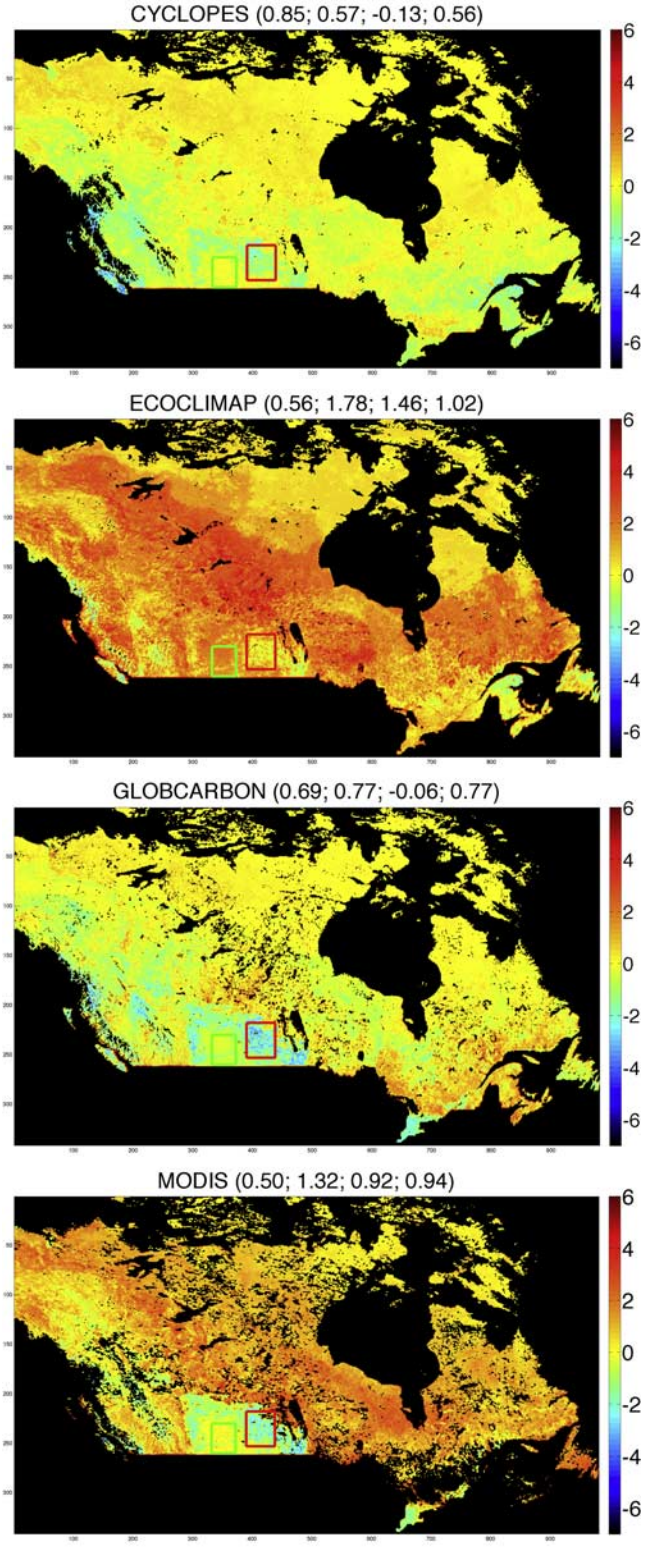

Figure 3. Map of Differences between each global LAI product under study and the CCRS regional LAI map over Canada for July 2003. The numbers shown in each figure's title respectively indicate the r^2, the RMSE, the bias (B), and the standard deviation of the difference (S) between the global product LAI values and the CCRS LAI values. The red square indicates the patches of mixed crop areas (corn, sorghum, canola) resolved by the CCRS LAI map but not by the global products. The green square represents the grassland and cereal crop areas where most global products are in agreement with the CCRS LAI map. The black pixels correspond to missing data, water or pixels out of the CCRS product geographic zone.

[33] ECOCLIMAP shows the largest spatial inconsistencies and positive bias (BIAS = 1.46) with the CCRS product due to interannual variations and disturbances (fires, ice-storms, insect damages, deforestation) over Canada between 1992 (date of the ECOCLIMAP climatology) and 2003. The highest consistency with the CCRS map is reached by CYCLOPES (RMSE = 0.57) followed by GLOBCARBON (RMSE = 0.77). CYCLOPES slightly overestimates CCRS LAI mainly over arctic vegetation (north of Canada) and underestimates it over boreal forest. The latter is due to the lack of clumping representation at the shoot scale in the CYCLOPES algorithm. GLOBCARBON shows contrasting results over Canadian forests with possible large overestimation over the boreal shield and the Atlantic maritime zone and underestimation over Pacific maritime and rocky zones, indicating possible uncertainties in the clumping index used in the GLOBCARBON algorithm. GLOBCARBON instability over forest will be confirmed by the temporal analysis in the section 5.1.2. Note, also, that GLOBCARBON shows systematic missing data in the center of Canada because the LAI was not estimated for pixels classified as "Burned forest" in the GLC2000 land cover map. A large positive bias ($B = 0.9$) is observed for MODIS over Canadian forests. This is mainly due to the lack of species based information on shoot structure in the MODIS LUTs [*Abuelgasim et al.*, 2006; *Rochdi et al.*, 2006], incorrect land cover labeling amplified by a high sensitivity of MODIS algorithm to vegetation class, and the lack of use of the SWIR band that was proven to improve LAI estimation over mixed forests with variable understory conditions [*Brown et al.*, 2000]. These figures also underline the very low spatial continuity of MODIS for which the main algorithm frequently fails over boreal Canadian forest (see section 5.1.2).

5.1.1.3. Vegetation Class Consistency

[34] To assess the discrepancies between the LAI products at the global scale, product versus product scatterplots are generated over the BELMANIP sites, using the LAI values from the 48 months of the 2001–2003 period, for each vegetation class under study (Figures 4–8).

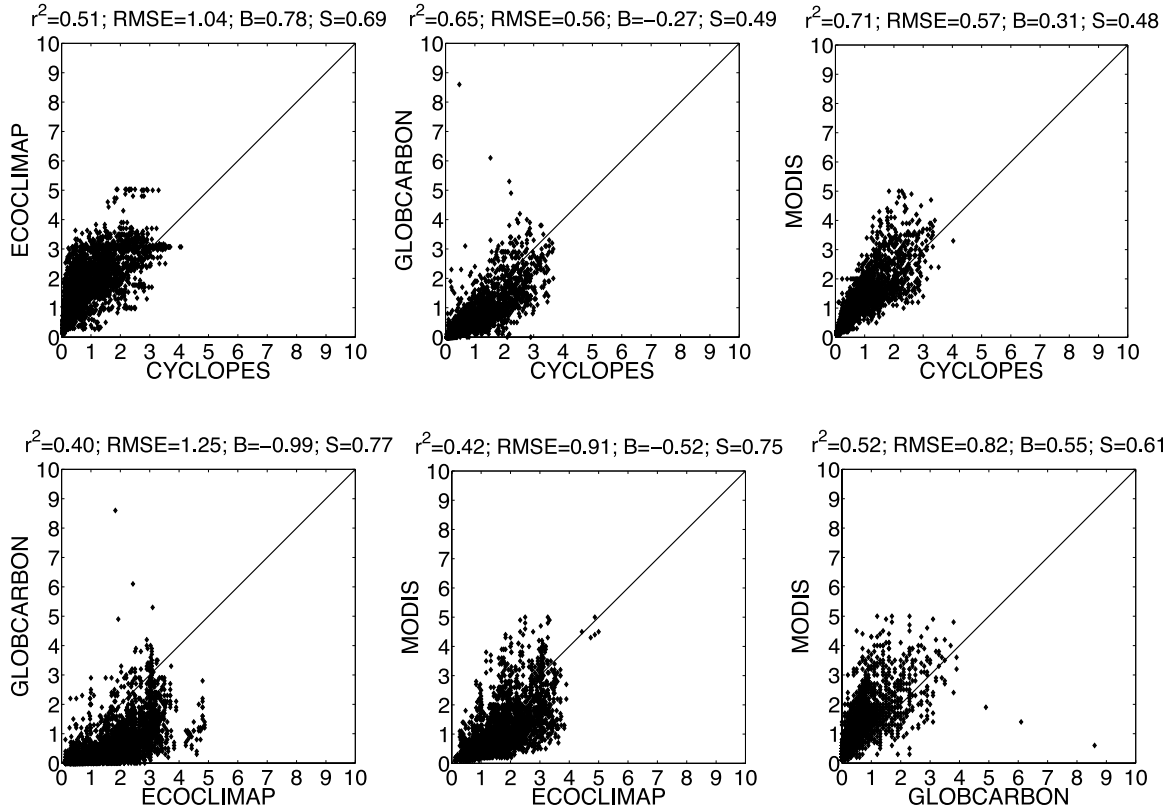

Figure 4. Product versus product scatterplots over the grassland BELMANIP sites, using the LAI values from the 48 months of the 2001–2003 period. The terms B and S represent the mean and the standard deviation of the difference between the LAI retrievals displayed in the *y* axis and those shown in the *x* axis.

[35] ECOCLIMAP provides much larger LAI estimates than the other products, however, with MODIS smaller discrepancies were found over forests. Note, in particular, that over grassland and cropland very low CYCLOPES, GLOBCARBON and MODIS LAI estimates can correspond to very high ECOCLIMAP LAI values. This reflects the lack of LAI interannual variations in the ECOCLIMAP algorithm.

[36] The best agreement between products is reached over grasslands and croplands (Figures 4 and 5) between CYCLOPES and GLOBCARBON (*RMSE* = 0.56 for grass and 0.74 for crops), and between MODIS and CYCLOPES (*RMSE* = 0.57 for grass and 0.65 for crops). We note, however, a slight bias between retrievals: MODIS > CYCLOPES > GLOBCARBON. Reasons for these biases are not obvious and can be due to differences in both the canopy models and/or the input surface reflectances, used in each retrieval algorithm. Indeed, *Verger et al.* [2008] have shown over all the BELMANIP sites during the 2002–2003 period that the CYCLOPES surface reflectances were between 5 and 8% lower than MODIS ones. Over croplands, the landscape clumping which is taken into account in both the CYCLOPES and MODIS algorithm but not in the GLOBCARBON algorithm may explain part of the lower GLOBCARBON LAI estimates.

[37] Over forests, MODIS provides much larger LAI estimates than CYCLOPES (*B* between 0.9 and 1.3) and GLOBCARBON (*B* between 0.9 and 1.2). Discrepancies between retrievals over forests reflect substantial differences in canopy structure modeling (e.g., clumping and understory) in each algorithm. Indeed, the early saturation of surface reflectance and the lack of clumping representation (at the plant and canopy scales) in the CYCLOPES algorithm [*Weiss et al.*, 2007] limit the range of LAI estimates (maximum value of 4) over forests (Figures 6–8). Since both MODIS and GLOBCARBON algorithms account for vegetation clumping at the shoot scale, positive biases between their LAI retrievals and those from CYCLOPES algorithm are expected over ENF. While this is verified for MODIS, differences between GLOBCARBON and CYCLOPES show large random fluctuations (*S* = 0.98 and *B* = 0) for LAI smaller than three (Figure 6). This may be due to either uncertainties in the clumping index used in the GLOBCARBON algorithm or other sources of error in the CYCLOPES and GLOBCARBON algorithms which cancel out the clumping effect. Very high LAI values (larger than 8) occasionally shown by GLOBCARBON are unrealistic for ENF targets at 1/11.2° GSD. Also, the low (less than 1) LAI values shown by MODIS, CYCLOPES and particularly GLOBCARBON are unrealistic for closed canopy ENF. This may be due to inadequate masking of clouds or snow.

[38] Over DBF (Figure 7), products are better correlated than over ENF, with particularly good agreement between CYCLOPES and GLOBCARBON (RMSE = 0.67). This is

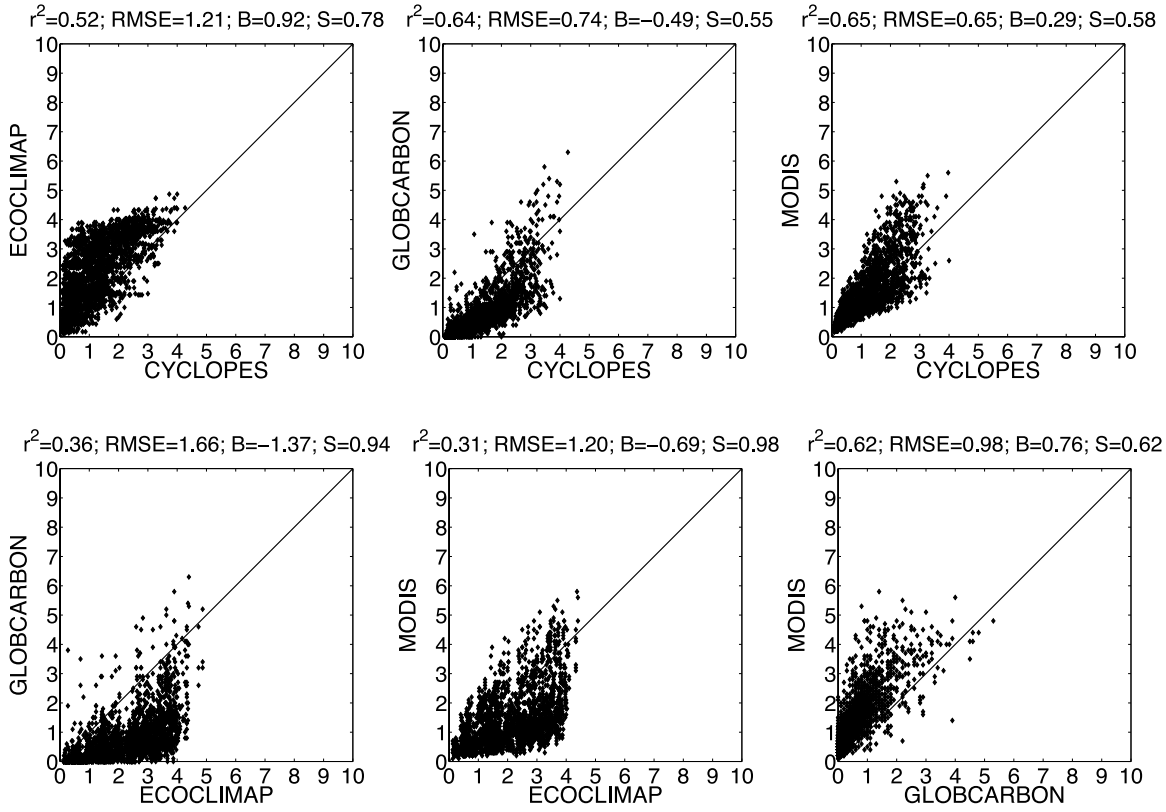

Figure 5. Product versus product scatterplots over the cropland BELMANIP sites, using the LAI values from the 48 months of the 2001–2003 period. The terms B and S represent the mean and the standard deviation of the difference between the LAI retrievals displayed in the *y* axis and those shown in the *x* axis.

mainly explained by the lower foliage clumping generally observed over DBF than over ENF.

[39] The most important discrepancies between retrievals are observed over EBF (RMSE between 1.22 and 2.80, Figure 8) due to saturation of the radiometric signal (at LAI∼4 for CYCLOPES and LAI∼6 for MODIS), residual atmospheric and cloud contamination as well as differences in canopy structure representation between algorithms. As over ENF, LAI estimates smaller than 1 (e.g., GLOBCARBON and CYCLOPES) are unrealistic for evergreen vegetation.

5.1.2. Temporal Consistency

[40] For their effective use in land surface models, LAI products should generally limit gaps in their time series. Thus, we first evaluate the temporal continuity (i.e., frequency of valid retrievals) of the products for each vegetation class over the BELMANIP sites during the period 2001–2003 (Table 3). MODIS shows the lowest temporal continuity, particularly over forest, followed by CYCLOPES, mainly due to cloud, atmospheric and snow contamination, or failure of the MODIS main algorithm over DBF. Note, that the wider temporal window used for compositing in the CYCLOPES algorithm (30 d), compared to the 8-d period used in the MODIS algorithm, reduces the frequency of missing data for CYCLOPES. ECOCLIMAP has by definition no missing data (the low amount of missing data over DBF is due to errors in the ECOCLIMAP water mask). In the GLOBCARBON algorithm, the post-processing gap filling and the concurrent use of observations from two sensors explain the lower frequency of missing data. Note, however, that GLOBCARBON data are systematically missing over some particular locations while other products provide valid data, such as the Altiplano in Bolivia (TURCO, sparse vegetation −18.24S; −68.19W), sites in Europe (e.g., Sonian, forest, 50.77N; 4.41E) among others, without obvious explanations.

[41] We now evaluate the consistency of the temporal trajectory of each product over selected BELMANIP sites (three per vegetation class) for the period 2001–2003 (Figure 9). For the Canadian sites, the global products are also compared to the CCRS regional reference. Thirteen of the 18 temporal plots display one or more LAI ground-based measurement, that is, the mean LAI reference map available over the site.

[42] Over grasslands (Figure 9a), the LAI products show similar temporal trajectories, however, with differences in magnitude. While the strongest agreement is achieved between CYCLOPES and MODIS as shown at Larzac, ECOCLIMAP shows the highest LAI value and GLOBCARBON the lowest. Note, however, that during the dry season at Gourma and Sevilleta, ECOCLIMAP and MODIS maintain higher LAI values than the more realistic low LAI values of CYCLOPES and GLOBCARBON. All the products, except ECOCLIMAP, properly capture interannual variability such as the decrease of LAI at Sevilleta in 2003 due to reduced precipitation, or the early drop of LAI at Larzac in 2003 due to a significant summer drought over western Europe. The temporal continuity of the products is

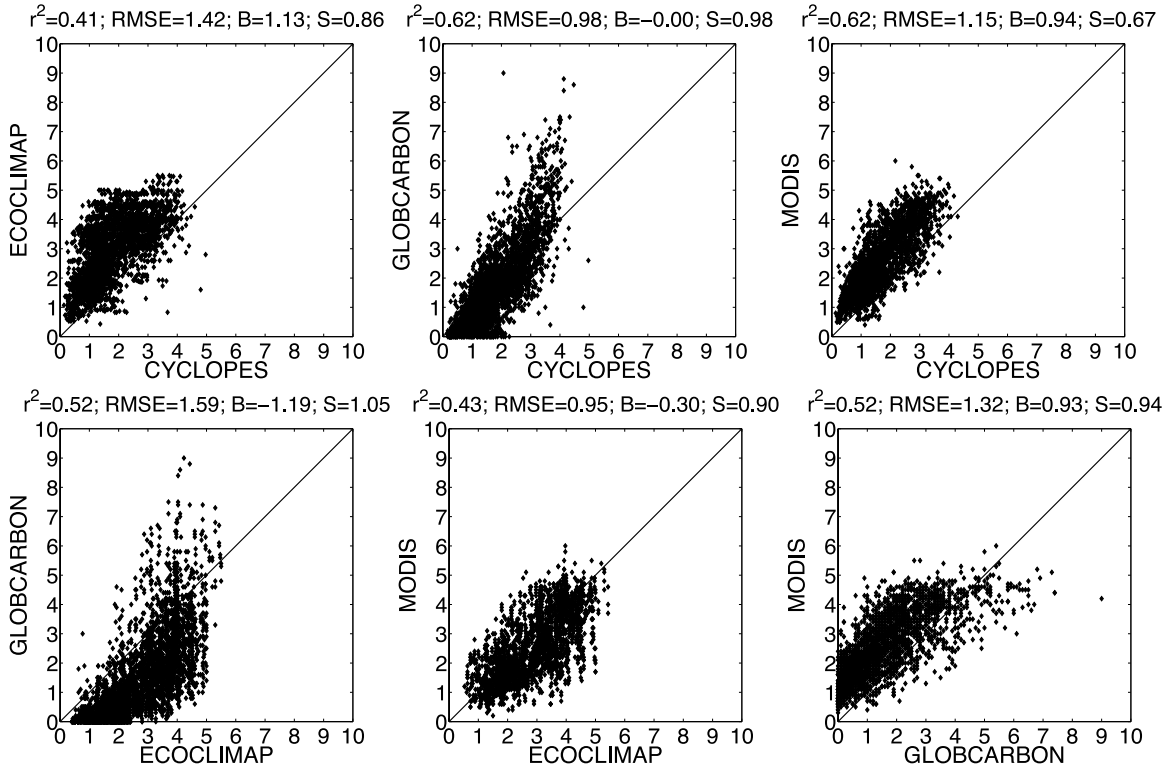

Figure 6. Product versus product scatterplots over the Evergreen Needleleaf Forest BELMANIP sites, using the LAI values from the 48 months of the 2001–2003 period. The terms B and S represent the mean and the standard deviation of the difference between the LAI retrievals displayed in the *y* axis and those shown in the *x* axis.

generally good, except for MODIS at Gourma, where the main algorithm fails frequently without an apparent reason.

[43] Over cropland (Figure 9b), all the products generally have realistic seasonal profiles. Note, however, that ECOCLIMAP cannot capture interannual variability and its seasonal trajectory can be completely shifted (e.g., Haouz) as compared to that of other products. MODIS, CYCLOPES, and GLOBCARBON agree well over Walnut Creek. However, the best agreement over most crop sites is achieved between CYCLOPES and MODIS, which are also the closest to ground measurements.

[44] Over ENF sites (Figure 9c), the products generally depict similar seasonal trajectories generated by the presence of understory (e.g., Nezer, Flakaliden) and/or broadleaf trees (e.g., Thompson site). Over Nezer and Flakaliden, most products describe low interannual variability, which is consistent for these sites. However, GLOBCARBON shows spurious temporal variations such as the drop of LAI over Nezer in summer of 2003, which is possibly due to residual cloud or atmospheric effects not corrected by the GLOBCARBON smoothing process. Over northern high latitude ENF sites (Thompson and Flakaliden), snow and cloud occurrence as well as low solar zenith angle in winter explain the lack of data for MODIS and CYCLOPES. The post-processing gap filling allows GLOBCARBON to provide LAI in winter over Thompson and Flakaliden, however, these value are too low (close to zero) to be realistic for an ENF site. The comparison to the CCRS product over Thompson indicates that during the growing season, MODIS, ECOCLIMAP, and GLOBCARBON frequently show too high LAI values to be representative of Canadian forests, where water bodies often cover a substantial portion of any given 1/11.2° grid cell [*Abuelgasim et al.*, 2006]. These figures also confirm the instability of GLOBCARBON product over ENF, whose magnitude can be as large as that of MODIS and ECOCLIMAP (Thompson) or lower than that of all the other products (Nezer, Flakaliden) despite the clumping included in its algorithm.

[45] The products also properly capture the seasonality of DBF sites (Figure 9d). They generally show smaller differences in magnitude than those observed over ENF, in particular for GLOBCARBON and CYCLOPES, which are very close to the CCRS product and the ground measurements (e.g., Larose). The MODIS LAI estimates are much larger than the other product estimates, especially in winter when the amount of vegetation is expected to be quasi null (except for Harvard and Larose which contain ENF). Besides, most MODIS main algorithm retrievals are frequently missing around the vegetation peak. As reported by *Shabanov et al.* [2005], the overestimation and failure of the MODIS main algorithm over broadleaf forest are due to inaccurate radiative transfer parameters (leaf albedo), lack of discrimination between EBF and DBF classes, and a high sensitivity of the retrieval algorithm to noise in surface reflectances (mainly aerosol contamination increasing in summer over northern high latitude forest) for large LAI (saturation domain). These figures also confirm the higher temporal instability of GLOBCARBON compared to the other products.

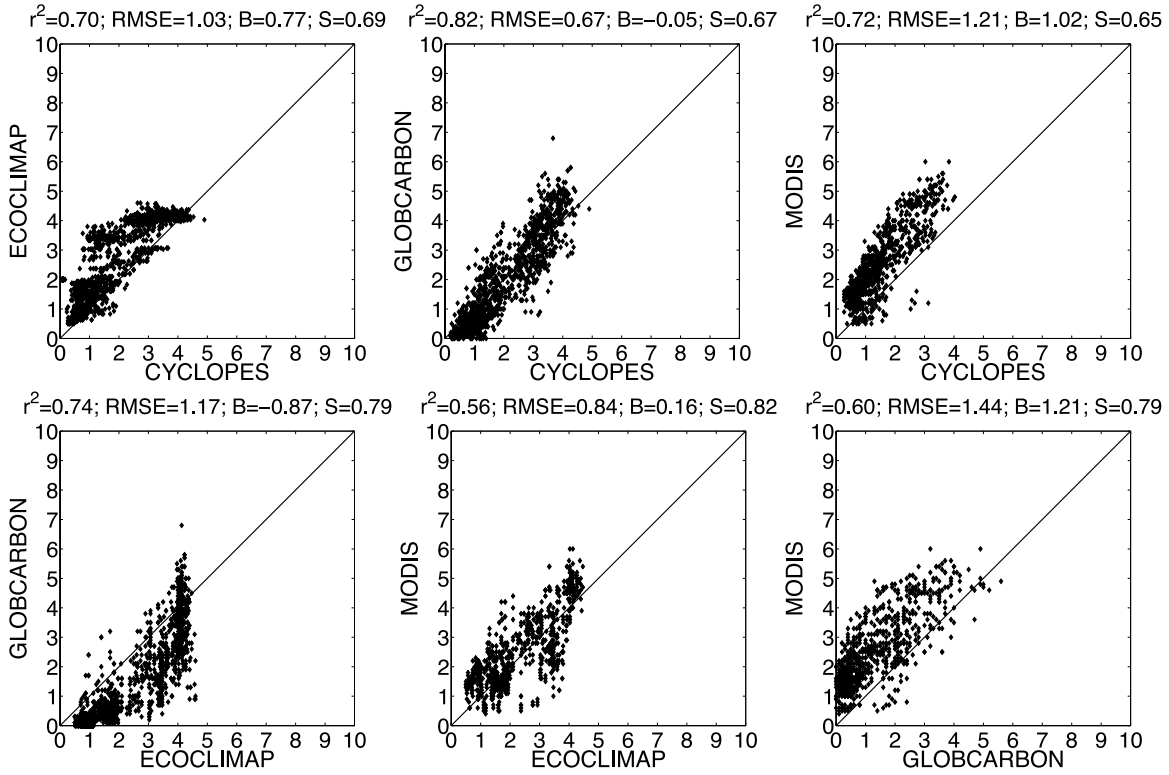

Figure 7. Product versus product scatterplots over the Deciduous Broadleaf Forest BELMANIP sites, using the LAI values from the 48 months of the 2001–2003 period. The terms B and S represent the mean and the standard deviation of the difference between the LAI retrievals displayed in the *y* axis and those shown in the *x* axis.

[46] The largest temporal inconsistencies are reached over EBF sites (Figure 9e). Because of high cloud occurrence, atmospheric contamination (aerosols), and saturation of the radiometric signal, CYCLOPES, and particularly MODIS, show poor temporal continuity. While seasonality is certainly lower over EBF than other biomes, it has been reported that vegetation amount temporally varies in relation with light availability and rainfall [*Xiao et al.*, 2006; *Myneni et al.*, 2007]. The ECOCLIMAP temporal trajectory is stable and continuous but does not show any seasonality over Tapajos and Counami. GLOBCARBON captures seasonal variations, which are, however, too large (minimum value too low) and too erratic (especially at Congo forest site) to be realistic, suggesting frequent failure of the post-processing gap filling.

5.2. Direct Validation

[47] In the previous sections, we have shown substantial differences in LAI magnitude between products. We further investigate this aspect by directly comparing each product with the LAI reference maps (Table 2) corrected for vegetation clumping (Figure 10). The number of validation points was similar for all the products, except for MODIS, which has much fewer valid data over mixed forest (see previous section). The uncertainty of each product is quantified by the RMSE computed over the same set of LAI reference maps for which all the products provide valid data.

[48] The lowest uncertainty is achieved by CYCLOPES (*RMSE* = 0.78) followed by GLOBCARBON (*RMSE* = 1.15) and MODIS (*RMSE* = 1.19). ECOCLIMAP shows the largest uncertainty (*RMSE* = 1.56) and generally overestimates the LAI reference maps, due to large uncertainties in the LAI measurements used in the ECOCLIMAP algorithm, poor description of surface spatial variability, poor performances of the AVHRR NDVI time series (in terms of radiometric calibration, geometry, atmospheric correction and cloud screening), and lack of interannual variations.

[49] In addition to the uncertainties in surface reflectance (mainly residual aerosol and cloud contamination) that can affect LAI retrievals of all the products over all vegetation classes, the accuracy of each product varies with vegetation class as explained below. Over cropland and grassland, CYCLOPES and MODIS are more accurate than GLOBCARBON which systematically underestimates the LAI reference maps. Note, however, that for one point, corresponding to a mixed forest and crop site (Gilching, see Table 2), all the products show large underestimation. This may be due to error in land cover labeling for MODIS, ECOCLIMAP, and GLOBCARBON for which this site is considered to be pure cropland. In general, mixed vegetation sites are not properly described by global LAI products. The lack of landscape clumping in the GLOBCARBON algorithm may explain part of its larger LAI underestimation over agricultural sites compared to CYCLOPES and MODIS.

[50] MODIS Collection 4 substantially overpredicts LAI over ENF and mixed forests confirming results from *Leuning et al.* [2005], *Abuelgasim et al.* [2006], *Cohen et*

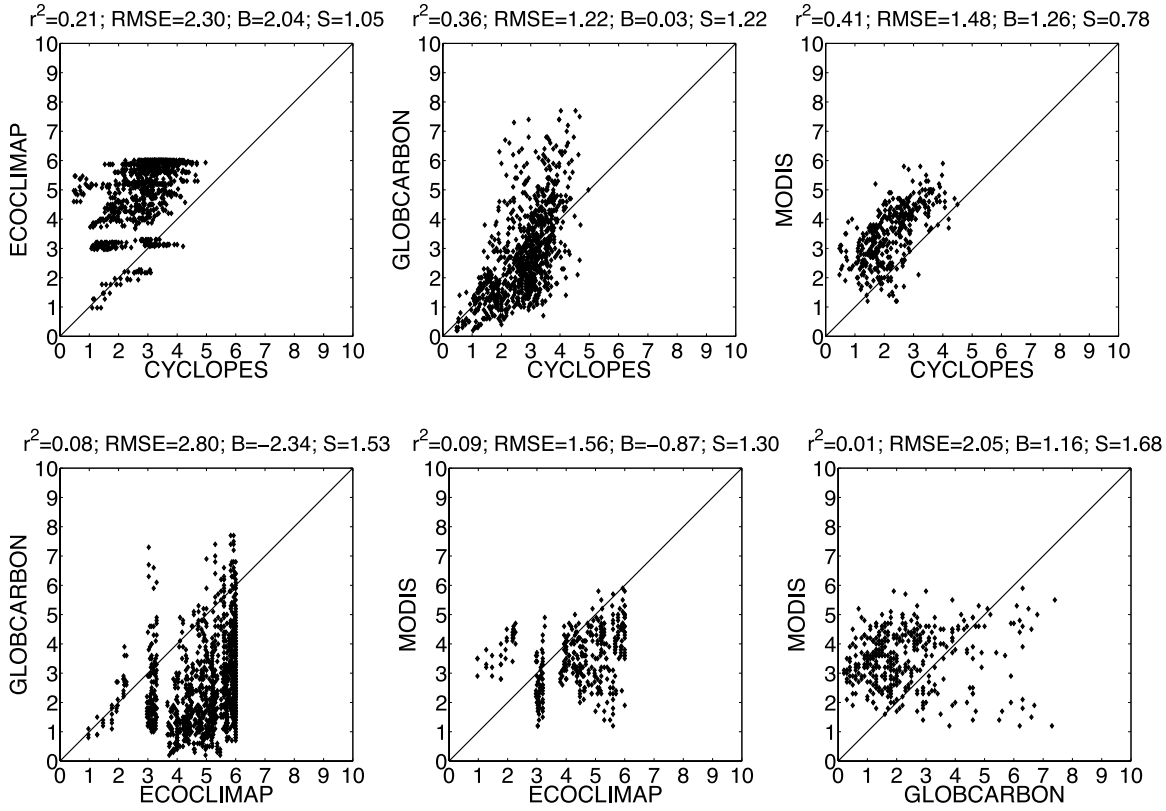

Figure 8. Product versus product scatterplots product over the Evergreen Broadleaf Forest BELMANIP sites, using the LAI values from the 48 months of the 2001–2003 period. The terms B and S represent the mean and the standard deviation of the difference between the LAI retrievals displayed in the *y* axis and those shown in the *x* axis.

al. [2006], *Ahl et al.* [2006], and *Weiss et al.* [2007]. The main reasons include the mismatch between simulated and measured MODIS surface reflectances (due to not optimal selection of radiative transfer parameters, especially spectral leaf albedo) and the high sensitivity of MODIS retrievals to surface reflectance uncertainties for large LAI [*Shabanov et al.*, 2005]. Besides, an additional source of uncertainty over forests is the lack of representation of mixed forest (particularly for MODIS and GLOBCARBON algorithms calibrated per vegetation type). CYCLOPES appears to be the most accurate product over ENF and particularly over mixed forest. However, this result is inconsistent with respect to the characteristics of the CYCLOPES algorithm, which does not include clumping at the shoot scale and thus should provide lower LAI estimates than the LAI reference maps. A possible reason for this is that most forest LAI reference maps do not account for the understory, partly cancelling out the clumping effect.

[51] Over EBF, all the products show significant uncertainties, generally underestimating ground measurements, due to reflectance saturation and cloud-aerosol contamination.

6. Discussion

[52] We first discuss some limitations in our results and then possible improvements for future LAI products.

6.1. Study Limitations

[53] Our validation results must be put into perspective given the uncertainties associated with ground measurements, particularly over forests [*Chen et al.*, 2006b]. Indeed, the differences in LAI uncertainty (see RMSE on Figure 10) between CYCLOPES, GLOBCARBON, and MODIS are smaller than 0.5 LAI, which is close to the typical bias error expected for most LAI reference maps (see section 4.2.2). Our results are particularly limited by possible lack of understory quantification in ground measurements, small number of measurements taking into account foliage clumping (see Table 2), uncertainty in clumping estimation, and

Table 3. Percentage of Missing Data Over the BELMANIP Sites During the 2001–2003 Period for Each Product Under Study[a]

Product	Total	Grass	Crop	ENF	DBF	EBF
CYCLOPES	19.3	18.3	10.1	27.6	16.8	26.3
ECOCLIMAP	1.2	0	0	0	2.2	0
GLOBCARBON	10.6	5.6	5.1	2.8	10.9	0
MODIS	37.9	25.7	20.4	41.2	44.9	69

[a]Total is displayed in the first column, while other columns provide results for each vegetation class.

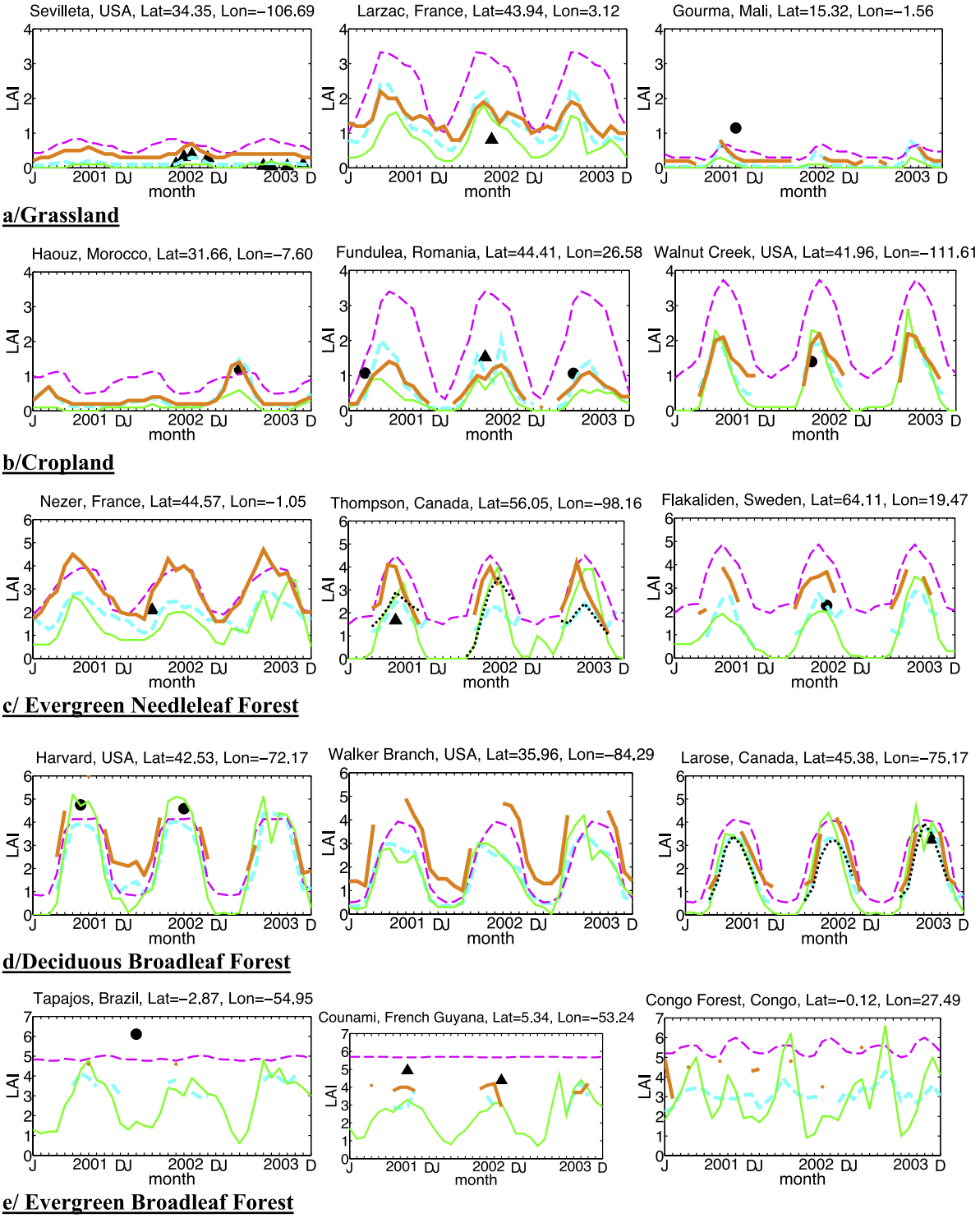

Figure 9. Interannual and seasonal variations of MODIS, GLOBCARBON, ECOCLIMAP, CYCLOPES, and CCRS (only over Canadian sites) LAI over some BELMANIP sites during the 2001–2003 period. Triangle (circle) represent ground LAI measurement corrected (not corrected) for clumping.

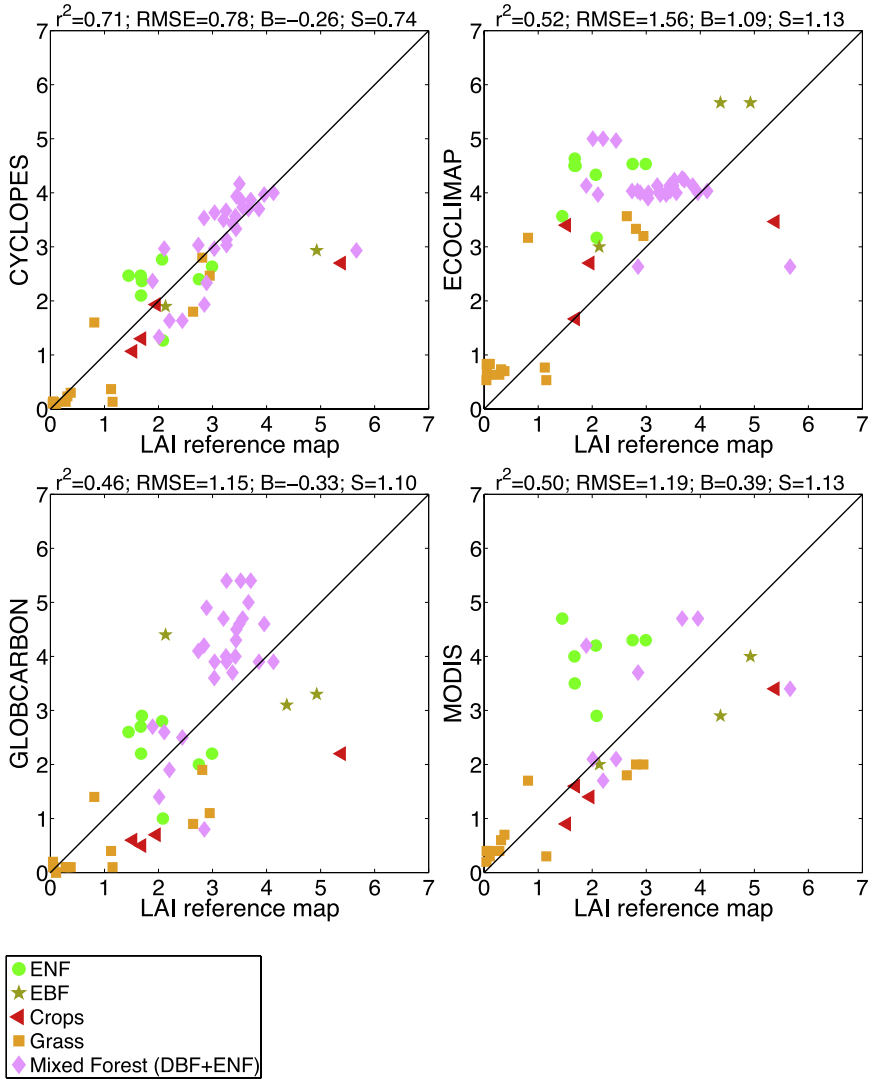

Figure 10. Direct validation results: comparison of each LAI product with the LAI reference maps corrected for clumping. 56 LAI reference maps were available for this comparison. The number of valid data are CYCLOPES = 57, ECOCLIMAP = 58, GLOBCARBON = 56, and MODIS = 36. RMSE, r^2, B and S are computed between the LAI products and the LAI reference maps using only those LAI reference maps for which all the products provide valid data.

saturation of optical measurements under evergreen broadleaf forest. These issues must be properly addressed by future validation works to improve the accuracy of LAI reference maps. Besides, the uncertainty in LAI reference maps, information lacking in current validation data sets, must be quantified in future fieldworks to properly validate global LAI products.

[54] The validation data set used in this work does not properly represent the global and seasonal variability of land surface types. Higher sampling rates are required for cropland, EBF, sparsely vegetated areas (e.g., woody savanna, open shrubland), permanent wetland sites, as well as for several regions (Africa, Eurasia, South America, Australia and Asia). Furthermore, to validate the seasonal variations of LAI products, continuous and automatic measurements of LAI should be developed.

[55] An additional source of uncertainty in our results is the possible spatial and temporal mismatch between the LAI reference maps and the moderate resolution products (see section 4.2.3). This particularly affects croplands since they are temporally and spatially more variable at the landscape scale than other vegetation classes [*Garrigues et al.*, 2006a, 2008a]. Note, however, that similar validation results have been found by *Weiss et al.* [2007] for CYCLOPES and MODIS which were evaluated over the same validation data set at 3 km GSD (close to the lowest size of the LAI reference maps) and a 10-d time step (closer to the field campaign date). This suggests that differences in spatial and temporal coverage between in situ data and LAI products may not have played a major role in our study.

[56] This exercise needs to be refined by evaluating the products at their native spatial (1 km) and temporal (∼8–10 d) sampling. This will ensure a better spatial and temporal consistency with validation data and will allow the evaluation of temporal smoothness and continuity of each product [*Weiss et al.*, 2007].

Table 4. Summary of Product Evaluation[a]

Criteria	CYCLOPES	ECOCLIMAP	GLOBCARBON	MODIS
Global distribution	+	–	+	+
Spatial consistency	+	–	–	+
Spatiotemporal continuity (i.e., no data gaps)	–	+	+	–
Temporal consistency (Interannual and seasonal variations)	+	–	–	+
Magnitude of LAI				
High values	–	+	+	+
Low values	+	+	+	–
Comparison with in-situ data	+	–	–	–

[a]The plus (minus) symbol means that the product has a good (poor) performance according to this criterion.

[57] This work should also be updated with any new version of LAI products, in particular MODIS Collection 5 due to be complete in 2008. In MODIS Collection 5, the LUTs of the LAI algorithm were recalculated based on a stochastic radiative transfer model to address 3D radiative transfer effects of spatial heterogeneity [*Shabanov et al.*, 2007; *Huang et al.*, 2008] and to achieve better radiometric consistency between simulated and MODIS surface reflectance [*Shabanov et al.*, 2005]. As a direct result, the amount of best quality main algorithm retrievals over forested regions increased by 10–15% globally and Collection 4 anomalies over DBF (overestimation through the year and failure in summer) and ENF (overestimation of seasonal peak) were minimized [*Yang et al.*, 2006c]. These improvements are still limited by the accuracy of input MODIS surface reflectance (particularly aerosols and snow contamination [*Yang et al.*, 2006a, 2006b, 2006c]). Our results will serve as a reference for assessing improvements in upcoming versions of LAI products including MODIS Collection 5, CYCLOPES version 4 and GLOBCARBON version 2 which will be validated and compared in a future paper.

6.2. LAI Product Improvements

[58] This study points out several aspects of current global LAI products that need to be improved. As demonstrated in this work, distinct LAI products derived from the same sensor (e.g., GLOBCARBON, CYCLOPES, and CCRS using SPOT/VEGETATION data) can be substantially different, suggesting the importance of the preprocessing steps applied to the radiometric data and the type of algorithm used to retrieve LAI. Since uncertainties in surface reflectance limit potential improvements in LAI retrieval, particular attention must be paid to radiometric calibration, atmospheric (aerosol) correction, cloud screening and view-illumination geometry normalization. The temporal and spatial continuity of LAI products must be improved by more accurate compositing, gap filling, and smoothing procedures [*Chen et al.*, 2006a; *Gao et al.*, 2008]. Algorithms based on multisensor observations should be further developed to extend the set of valid remote sensing observations [*Yang et al.*, 2006a, 2006b, 2006c; *Verger et al.*, 2008]. Global algorithms should also better describe the spatial and temporal variability of vegetation structure with emphasis on foliage clumping at the plant and canopy scales. A possible option could be to correct the LAI assessment by applying a clumping index derived from multiangular surface reflectance measurements [*Lacaze et al.*, 2003; *Chen et al.*, 2005]. Since current coarse resolution observations are limited to describe mixed biomes, high spatial (20 m–100 m) and temporal (1–10 d) sampling remote sensing observations must be developed to better capture surface spatial heterogeneity, particularly over agricultural sites [*Garrigues et al.*, 2008a]. Finally, global algorithms could be supplemented by multiple regional algorithms calibrated using intensive field measurements over particular regions or ecosystems, as currently applied over Canada.

7. Conclusion

[59] In this study, the performances of four global LAI satellite products were evaluated at 1/11.2° spatial sampling and a monthly time step: ECOCLIMAP climatology, GLOBCARBON (from SPOT/VEGETATION and ATSR/AATSR observations), CYCLOPES (from SPOT/VEGETATION data), and MODIS Collection 4 (main algorithm, from MODIS/TERRA observations). These products were spatially and temporally intercompared for the 2001–2003 period using the BELMANIP network of sites, which represents the global variability of land surface types. Their uncertainties were assessed by direct comparison with 56 LAI reference maps that were independently derived from ground measurements and concurrent high spatial resolution data. The comparisons were made according to several criteria of performance, leading to the general conclusions summarized in Table 4.

[60] First, all the products, except ECOCLIMAP, depict very smooth and continuous LAI value distributions as expected at global scale. CYCLOPES and MODIS show consistent spatial variations at continental scale, while ECOCLIMAP poorly describes surface spatial heterogeneity and GLOBCARBON tends to display erratic variations not directly linked to surface properties. However, these global products have difficulties in capturing some specific spatial patterns, as those displayed over Canada, that are well depicted by the CCRS regional algorithm because of its finer characterization of both mixed Canadian forest and land use variability.

[61] One of the most important criteria for using a satellite product in land surface models is its spatiotemporal continuity (i.e., no data gaps) and consistency. ECOCLIMAP is the only product that does not have spatiotemporal gaps. GLOBCARBON is also characterized by high spatiotemporal continuity despite some systematic missing data at particular locations. Conversely, MODIS and CYCLOPES tend to exhibit poor spatiotemporal continuity, especially in

winter over the northern high latitudes (due to cloud and snow coverage and low solar zenith angle), and over the equatorial belt (because of cloud cover). Over deciduous broadleaf forests, MODIS main algorithm frequently fails during the growing season and overestimates LAI throughout the year. This is mainly due to high sensitivity of MODIS main algorithm to noise in surface reflectances at large LAI, mismatch between simulated and measured MODIS surface reflectances, and lack of discrimination between deciduous and evergreen broadleaf forests. Note that these issues are now addressed in MODIS Collection 5. While ECOCLIMAP does not describe interannual LAI variations, CYCLOPES, MODIS, and GLOBCARBON show consistent temporal profiles with realistic seasonal and interannual variations over all vegetation types, except evergreen broadleaf forest. Note, however, that GLOBCARBON is inclined to display spurious temporal variations during the growing season over forests.

[62] All the products demonstrate an adequate dynamic range of retrieved LAI, except CYCLOPES, for which the retrieved LAI range is limited to 0–4 (due to early saturation and lack of clumping representation in the algorithm). This results in LAI underestimation for CYCLOPES over dense vegetation (forests). Note, however, that GLOBCARBON locally exhibits unrealistic high values for evergreen needleleaf forest at 10 km GSD. All the products consistently provide low LAI over sparsely vegetated areas or during the dormant season, except MODIS, which displays unrealistic high values. The low values shown by most products over high latitude evergreen needleleaf forests in winter are also not realistic and reflect the impact of low solar zenith angle, snow, and cloud contamination. The comparison between retrievals indicates large positive bias between ECOCLIMAP and the others products. CYCLOPES, MODIS, and GLOBCARBON LAI values agree better over croplands and grasslands than over forests, where differences in representation of vegetation structure (e.g., foliage clumping, understory) and leaf optical properties between algorithms, as well as high sensitivity to surface reflectance uncertainties, lead to substantial LAI discrepancies between products.

[63] This analysis indicates that CYCLOPES is the most similar product to the LAI reference maps, despite the lack of leaf clumping representation in the CYCLOPES algorithm. It also shows that MODIS and CYCLOPES are the most accurate over grass and crops and confirms the well-known overestimation of MODIS Collection 4 over deciduous broadleaf and needleleaf forests. Large uncertainties are observed for all the products over evergreen broadleaf forests due to highly saturated and contaminated surface reflectances. However, the direct validation results, reported here, must be put into perspective given the uncertainties in ground measurements (primarly understory and clumping estimation), the poor description of global and seasonal variability of land surface types and the possible spatial and temporal coverage mismatch between validation data and satellite products.

[64] Finally, the validation and intercomparison framework presented in this paper can be used for the evaluation of other remote sensing products such as albedo, fPAR, and surface temperature. This exercise is critical for the proper use of remote sensing products in land surface model as well for their consistent and continuous integration into climatic data records, both requiring updated and accurate validation results.

[65] **Acknowledgments.** Garrigues and Morisette's efforts were supported by NASA's Terrestrial Ecology Program (Diane Wickland, program manager) under grant 03-0408-0637. Special thanks are given to the participants of the CEOS LPV global LAI-Intercomparison activity. It is through the collaboration fostered by LPV that the reference LAI data sets were available for this study. In particular, we are grateful to all the groups referenced in the caption for Table 2.

References

Abuelgasim, R. A., R. A. Fernandes, and S. G. Leblanc (2006), Evaluation of national and global LAI products derived from optical remote sensing instruments over Canada, *IEEE Trans. Geosci. Remote Sens.*, *42*(7), 1872–1884.

Ahl, D. E., S. N. Gower, S. N. Burrows, N. V. Shabanov, R. B. Myneni, and Y. Knyazikhin (2006), Monitoring spring canopy phenology of a deciduous broadleaf forest using MODIS, *Remote Sens. Environ.*, *104*(1), 88–95.

Anderson, M. C., C. M. U. Neale, F. Li, J. M. Norman, W. P. Kustas, H. Jayanthi, and J. Chavez (2004), Upscaling ground observations of vegetation water content, canopy height, and leaf area index during SMEX02 using aircraft and Landsat imagery, *Remote Sens. Environ.*, *92*(4), 447–464.

Aragao, L. E. O. C., Y. E. Shimabukuro, F. D. B. Espirito-Santo, and M. Williams (2005), Spatial validation of the Collection 4 MODIS LAI product in eastern Amazonia, *IEEE Trans. Geosci. Remote Sens.*, *43*(11), 2526–2534.

Arora, V. (2002), Modeling vegetation as a dynamic component in soil-vegetation-atmosphere transfer schemes and hydrological models, *Rev. Geophys.*, *40*(2), 1006, doi:10.1029/2001RG000103.

Bacour, C., F. Baret, D. Beal, M. Weiss, and K. Pavageau (2006), Neural network estimation of LAI, fAPAR, fCover and LAIxCab, from top of canopy MERIS reflectance data: Principles and validation, *Remote Sens. Environ.*, *105*(4), 313–325.

Barclay, H. J., J. A. Trofymow, and R. I. Leach (2000), Assessing bias from boles in calculating leaf area index in immature Douglas-fir with the LI-COR canopy analyzer, *Agric. For. Meteorol.*, *100*(2–3), 255–260.

Baret, F., and G. Guyot (1991), Potentials and limits of vegetation indices for LAI and FAPAR assessment, *Remote Sens. Environ.*, *35*, 161–173.

Baret, F., et al. (2006), Evaluation of the representativeness of networks of sites for the global validation and inter-comparison of land biophysical products: Proposition of the CEOS-BELMANIP, *IEEE Trans. Geosci. Remote Sens.*, *42*(7), 1794–1803.

Baret, F., et al. (2007), LAI, fAPAR and fCover CYCLOPES global products derived from VEGETATION: Part 1: Principles of the algorithm, *Remote Sens. Environ.*, *110*, 275–286.

Baret, F., et al. (2008), VALERI: A network of sites and a methodology for the validation of medium spatial resolution land satellite product, *Remote Sens. Environ.*, in press.

Bartholome, E., and A. Belward (2005), GLC2000: A new approach to global land cover mapping from Earth Observation data, *Int. J. Remote Sens.*, *26*(9), 1959–1977.

Brown, L., J. M. Chen, S. G. Leblanc, and J. Cihlar (2000), A shortwave infrared modification to the simple ratio for LAI retrieval in boreal forests: An image and model analysis, *Remote Sens. Environ.*, *71*, 16–25.

Buermann, W., J. Dong, X. Zeng, R. B. Myneni, and R. E. Dickinson (2001), Evaluation of the utility of satellite-based vegetation leaf area index data for climate simulations, *J. Clim.*, *14*(17), 3536–3550.

Buermann, W., Y. Wang, J. Dong, L. Zhou, X. Zeng, R. E. Dickinson, C. S. Potter, and R. B. Myneni (2002), Analysis of a multiyear global vegetation leaf area index data set, *J. Geophys. Res.*, *107*(D22), 4646, doi:10.1029/2001JD000975.

Butson, C. R., and R. A. Fernandes (2004), A consistency analysis of surface reflectance and leaf area index retrieval from overlapping clear-sky Landsat ETM+ imagery, *Remote Sens. Environ.*, *89*(3), 369–380.

Cayrol, P., L. Kergoat, S. Moulin, G. Dedieu, and A. Chehbouni (2000), Calibrating a coupled SVAT- vegetation growth model with remotely sensed reflectance and surface temperature a case study for the Hapex-Sahel grassland sites, *J. Appl. Meteorol.*, *39*(12), 2452–2472.

Chen, J. (1999), Spatial scaling of a remotely sensed surface parameter by contexture, *Remote Sens. Environ.*, *69*, 30–42.

Chen, J. M., and T. A. Black (1992), Defining leaf area index for non-flat leaves, *Plant Cell Environ.*, *15*, 421–429.

Chen, J. M., and J. Cihlar (1995), Quantifying the effect of canopy architecture on optical measurements of leaf area index using two gap size method analysis, *IEEE Trans. Geosci. Remote Sens.*, *33*(3), 777–787.

Chen, J. M., and S. Leblanc (2001), Multiple-scattering scheme useful for hyperspectral geometrical optical modelling, *IEEE Trans. Geosci. Remote Sens.*, *39*(5), 1061–1071.

Chen, J. M., P. Rich, S. T. Gower, J. M. Norman, and S. Plummer (1997), Leaf area index of boreal forests: Theory, techniques and measurements, *J. Geophys. Res.*, *102*(D24), 29,429–29,443.

Chen, J. M., G. Pavlic, L. Brown, J. Cihlar, S. G. Leblanc, H. P. White, R. J. Hall, D. R. Peddle, D. J. King, and J. A. Trofymow (2002), Derivation and validation of Canada-wide coarse-resolution leaf area index maps using high-resolution satellite imagery and ground measurements, *Remote Sens. Environ.*, *80*(1), 165–184.

Chen, J. M., C. H. Menges, and S. Leblanc (2005), Global derivation of the vegetation clumping index from multi-angular satellite data, *Remote Sens. Environ.*, *97*, 447–457.

Chen, J. M., F. Deng, and M. Chen (2006a), Locally adjusted cubic-spline capping for reconstructing seasonal trajectories of a satellite-derived surface parameter, *IEEE Trans. Geosci. Remote Sens.*, *44*(12), 3725–3736.

Chen, J. M., A. Govind, O. Sonnentag, Y. Zhang, A. Barr, and B. Amiro (2006b), Leaf area index measurements at Fluxnet-Canada forest sites, *Agric. For. Meteorol.*, *140*(1–4), 257–268.

Cihlar, J., R. Latifovic, J. Beaubien, B. Guindon, and M. Palmer (2003), Thematic mapper (TM) based accuracy assessment of a land cover product for Canada derived from SPOT VEGETATION (VGT) data, *Can. J. Rem. Sens.*, *29*(2), 154–170.

Cohen, W. B., T. K. Maiersperger, D. P. Turner, W. D. Ritts, D. Pflugmacher, R. E. Kennedy, A. A. Kirschbaum, S. W. Running, M. Costa, and S. T. Gower (2006), MODIS land cover and LAI Collection 4 product quality across nine sites in the western hemisphere, *IEEE Trans. Geosci. Remote Sens.*, *44*(7), 1843–1858.

Combal, B., F. Baret, M. Weiss, A. Trubuil, D. Macé, A. Pragnère, R. Myneni, Y. Knyazikhin, and L. Wang (2002), Retrieval of canopy biophysical variables from bi-directional reflectance data. Using prior information to solve the ill-posed inverse problem, *Remote Sens. Environ.*, *84*, 1–15.

Deng, F., J. M. Chen, S. Plummer, M. Chen, and J. Pisek (2006), Global LAI algorithm integrating the biderectional information, *IEEE Trans. Geosci. Remote Sens.*, *44*, 2219–2229.

Dickinson, R. E. (1995), Land processes in climate models, *Remote Sens. Environ.*, *51*, 27–38.

Eriksson, H., L. Eklundh, A. Kuusk, and T. Nilson (2006), Impact of understory vegetation on forest canopy reflectance and remotely sensed LAI estimates, *Remote Sens. Environ.*, *103*, 408–418.

Fernandes, R., H. P. White, S. Leblanc, G. Pavlic, H. McNairn, J. M. Chen, and R. J. Hall (2001), Examination of error propagation in relationships between leaf area index and spectral vegetation indices from Landsat-5 TM and Landsat-7 ETM+, paper presented at 23rd Canadian Remote Sensing Symposium, Quebec City, Quebec, 21–24 Aug.

Fernandes, R. A., C. Butson, S. Leblanc, and R. Latifovic (2003), A, Landsat-5 TM and Landsat-7ETM+ based accuracy assessment of leaf area index products for Canada derived from SPOT4/VGT data, *Can. J. Rem. Sens.*, *29*(2), 241–258.

Friedl, M. A., D. K. McIver, J. C. F. Hodges, X. Y. Zhang, D. Muchoney, A. H. Strahler, C. E. Woodcock, S. Gopal, A. Schneider, and A. Cooper (2002), Global land cover mapping from MODIS: Algorithms and early results, *Remote Sens. Environ.*, *83*(1–2), 287–302.

Gao, F., J. Morisette, R. Wolfe, G. Ederer, J. Pedelty, E. Masuoka, R. Myneni, B. Tan, and J. Nightingale (2008), An algorithm to produce temporally and spatially continuous MODIS-LAI time series, *IEEE Trans. Geosci. Remote Sens.*, in press.

Garrigues, S., D. Allard, F. Baret, and M. Weiss (2006a), Quantifying spatial heterogeneity at the landscape scale using variogram models, *Remote Sens. Environ.*, *103*, 81–96.

Garrigues, S., D. Allard, and F. Baret (2006b), Influence of the spatial heterogeneity on the non linear estimation of Leaf Area Index from moderate resolution remote sensing data, *Remote Sens. Environ.*, *106*, 286–298.

Garrigues, S., D. Allard, and F. Baret (2008a), Modeling temporal changes in surface spatial heterogeneity over an agricultural site, *Remote Sens. Environ.*, *112*(2), 588–602.

Garrigues, S., N. Shabanov, K. Swanson, J. Morisette, F. Baret, and R. Myneni (2008b), Intercomparison and sensitivity analysis of Leaf Area Index retrievals from LAI-2000, AccuPAR, and digital hemispherical photography over croplands, *Agric. For. Meteorol.*, in press.

Gibelin, A.-L., J.-C. Calvet, J.-L. Roujean, L. Jarlan, and S. Los (2006), Ability of the land surface model ISBA-A-gs to simulate leaf area index at the global scale: Comparison with satellites products, *J. Geophys. Res.*, *111*, D18102, doi:10.1029/2005JD006691.

Goel, N. (1989), Inversion of canopy reflectance models for estimation of biophysical parameters from reflectance data, in *Theory and Applications of Optical Remote Sensing*, edited by G. Asrar, pp. 205–250, Wiley, New York.

Gower, S. T., C. J. Kucharik, and J. M. Norman (1999), Direct and indirect estimation of Leaf Area Index, FAPAR, and Net Primary Production of terrestrial ecosystems, *Remote Sens. Environ.*, *70*(1), 29–51.

Hagolle, O., A. Lobo, P. Maisongrande, F. Cabot, B. Duchemin, and A. De Pereyra (2005), Quality assessment and improvement of temporally composited products of remotely sensed imagery by combination of VEGETATION 1 and 2 images, *Remote Sens. Environ.*, *94*(2), 172–186.

Hu, J., B. Tan, N. Shabanov, K. A. Crean, J. V. Martonchik, D. J. Diner, Y. Knyazikhin, and R. B. Myneni (2003), Performance of the MISR LAI and FPAR algorithm: A case study in Africa, *Remote Sens. Environ.*, *88*(3), 324–340.

Huang, D., et al. (2007), Canopy spectral invariants for remote sensing and model applications, *Remote Sens. Environ.*, *106*, 106–122.

Huang, D., Y. Knyazikin, W. Wang, D. W. Deering, P. Stenberg, N. Shabanov, B. Tan, and R. B. Myneni (2008), Stochastic transport theory for investigating the three-dimensional canopy structure from space measurements, *Remote Sens. Environ.*, *112*(1), 35–50.

Iiames, J. S., A. N. Pilant, and T. E. Lewis (2004), In-situ estimates of forest LAI for MODIS data validation, in *Remote Sensing and GIS Accuracy Assessment*, edited by R. S. Lunetta and J. G. Lyon, pp. 41–58, CRC, Boca Raton, Fla.

Jonckheere, I., S. Fleck, K. Nackaerts, B. Muys, P. Coppin, M. Weiss, and F. Baret (2004), Review of methods for in situ leaf area index determination: Part I. Theories, sensors and hemispherical photography, *Agric. For. Meteorol.*, *121*(1–2), 19–35.

Justice, C., A. Belward, J. Morisette, P. Lewis, J. Privette, and F. Baret (2000), Developments in the validation of satellite sensor products for the study of the land surface, *Int. J. Remote Sens.*, *21*(17), 1251–1278.

Kalacska, M., G. A. Sanchez-Azofeifa, B. Rivard, J. C. Calvo-Alvarado, A. R. P. Journet, J. P. Arroyo-Mora, and D. Ortiz-Ortiz (2004), Leaf area index measurements in a tropical moist forest: A case study from Costa Rica, *Remote Sens. Environ.*, *91*, 134–152.

Kalacska, M., J. C. Calvo-Alvarado, and G. A. Sanchez-Azofeifa (2005a), Calibration and assessment of seasonal changes in leaf area index of a tropical dry forest in different stages of succession, *Tree Physiol.*, *25*, 733–744.

Kalacska, M., G. A. Sanchez-Azofeifa, J. C. Calvo-Alvarado, B. Rivard, and M. Quesada (2005b), Effects of season and succesional stage on leaf area index and spectral vegetation indices in three Mesoamerican tropical dry forests, *Biotropica*, *37*, 486–496.

Knyazikhin, Y., J. V. Martonchik, R. B. Myneni, D. J. Diner, and S. W. Running (1998), Synergistic algorithm for estimating vegetation canopy leaf area index and fraction of absorbed photosynthetically active radiation from MODIS and MISR data, *J. Geophys. Res.*, *103*(D24), 32,257–32,275.

Kucharik, C. J., J. M. Norman, and S. T. Gower (1998), Measurements of branch area and adjusting leaf area index indirect measurements, *Agric. For. Meteorol.*, *91*(1–2), 69–88.

Lacaze, R. (2005), POLDER-2 land surface level-3 products user manual: Algorithm description and product validation, technical report, Medias-France/POSTEL, Toulouse, France. (Available at http://smsc.cnes.fr/POLDER/SCIEPROD/P2-TE3-UserManual-I1.40.pdf)

Lacaze, R., J. M. Chen, J. J. Roujean, and S. Leblanc (2003), Retrieval of vegetation clumping index using hot spot signatures measured by POLDER instrument, *Remote Sens. Environ.*, *88*, 84–95.

Latifovic, R., Z.-L. Zhu, J. Cihlar, C. Giri, and I. Olthof (2004), Land cover mapping of North and Central America - Global Land Cover 2000, *Remote Sens. Environ.*, *89*(1), 116–127.

Leblanc, S. G., and J. M. Chen (2001), A practical scheme for correcting multiple scattering effects on optical LAI measurements, *Agric. For. Meteorol.*, *110*(2), 125–139.

Leuning, R., H. A. Cleugh, S. J. Zegelin, and D. Hughes (2005), Carbon and water fluxes over a temperate Eucalyptus forest and tropical wet/dry savanna in Australia: Measurements and comparison with MODIS remote sensing estimates, *Agric. For. Meteorol.*, *129*, 153–173.

Los, S. O., G. J. Collatz, P. J. Sellers, C. M. Malmstroem, N. H. Pollack, R. S. DeFries, L. Bounoua, M. T. Parris, C. J. Tucker, and D. A. Dazlich (2000), A global 9-year biophysical land surface data set from NOAA AVHRR data, *J. Hydrometeorol.*, *1*, 183–199.

Masson, V., J. L. Champeaux, F. Chauvin, C. Meriguer, and R. Lacaze (2003), A global database of land surface parameters at 1 km resolution in meteorological and climate models, *J. Clim.*, *16*, 1261–1282.

Morisette, J. T., et al. (2006), Validation of global moderate-resolution LAI Products: A framework proposed within the CEOS Land Product Validation subgroup, *IEEE Trans. Geosci. Remote Sens.*, *44*, 1804–1814.

Moulin, S., A. Bondeau, and R. Delécolle (1998), Combining agricultural crop models and satellite observations: From field to regional scales, *Int. J. Remote Sens.*, *19*(6), 1021–1036.

Muñoz, J., C. Rudiger, J.-C. Calvet, N. Fritz, L. Jarlan, and Y. Kerr (2008), Joint assimilation of surface soil moisture and LAI observations into a land surface model, *Agric. For. Meteorol.*, in press.

Myneni, R. B., F. G. Hall, P. J. Sellers, and A. L. Marshak (1995), The interpretation of spectral vegetation indices, *IEEE Trans. Geosci. Remote Sens.*, *33*, 481–486.

Myneni, R. B., R. R. Nemani, and S. W. Running (1997), Estimation of global leaf area index and absorbed par using radiative transfer models, *IEEE Trans. Geosci. Remote Sens.*, *35*, 1380–1393.

Myneni, R. B., et al. (2002), Global products of vegetation leaf area and fraction absorbed PAR from one year of MODIS data, *Remote Sens. Environ.*, *83*, 214–231.

Myneni, R. B., et al. (2007), Large seasonal swings in leaf area of Amazon rainforests, *Proc. Natl. Acad. Sci., Biol. Sci.: Ecol. Environ. Sci.*, 4820–4823.

Nemani, R. R., C. D. Keeling, H. Hashimoto, W. M. Jolly, S. C. Piper, C. J. Tucker, R. B. Myneni, and S. W. Running (2003), Climate-driven increases in global terrestrial net primary production from 1982 to 1999, *Science*, *300*, 1560–1563.

Nilson, T. (1971), A theoretical analysis of the frequency gaps in plant stands, *Agric. For. Meteorol.*, *8*, 25–28.

Pisek, J., and J. M. Chen (2007), Comparison and validation of MODIS and VEGETATION global LAI products over four BigFoot sites in North America, *Remote Sens. Environ.*, *109*(1), 81–94.

Privette, J. L., R. B. Myneni, Y. Knyazikhin, M. Mukufute, G. Roberts, Y. Tian, Y. Wang, and S. G. Leblanc (2002), Early spatial and temporal validation of MODIS LAI product in Africa, *Remote Sens. Environ.*, *83*, 232–243.

Rochdi, N., R. Fernandes, and M. Chelle (2006), An assessment of needles clumping within shoots when modeling radiative transfer within homogeneous canopies, *Remote Sens. Environ.*, *102*, 116–134.

Roujean, J. L., and R. Lacaze (2002), Global mapping of vegetation parameters from POLDER multiangular measurements for studies of surface-atmosphere interactions: A pragmatic method and validation, *J. Geophys. Res.*, *107*(D12), 4150, doi:10.1029/2001JD000751.

Running, S. W., D. Baldocchi, D. P. Turner, S. T. Gower, P. S. Bakwin, and K. A. Hibbard (1999), A global terrestrial monitoring network integrating tower fluxes, flask sampling, ecosystem modeling and EOS satellite data, *Remote Sens. Environ.*, *70*, 108–127.

Sellers, P. J. (1997), Modeling the exchange of energy, water, and carbon between continents and atmosphere, *Science*, *275*, 602–609.

Sellers, P. J., S. O. Los, C. J. Tucker, C. O. Justice, D. A. Dazlich, G. J. Collatz, and D. A. Randall (1996), A revised land surface parameterization (SiB2) for atmospheric GCMS. Part II: The generation of global fields of terrestrial biophysical parameters from satellite data, *J. Clim.*, *9*(4), 706–737.

Shabanov, N. V., et al. (2005), Analysis and optimization of the MODIS Leaf Area Index algorithm retrievals over broadleaf forests, *IEEE Trans. Geosci. Remote Sens.*, *43*(8), 1855–1865.

Shabanov, N. V., D. Huang, Y. Knyazikhin, R. E. Dickinson, and R. B. Myneni (2007), Stochastic radiative transfer model for mixture of discontinuous vegetation canopies, *J. Quant. Spectrosc. Radiat. Transf.*, *107*(2), 236–262.

Stenberg, P. (1996), Correcting LAI2000 estimates for the clumping of needles in shoots of conifers, *Agric. For. Meteorol.*, *43*, 20–34.

Stenberg, P., T. Nilson, S. Smolander, and P. Voipio (2003), Gap fraction based estimation of LAI in scots pine stands subjected to experimental removal of branches and stems, *Can. J. Rem. Sens.*, *29*, 363–370.

Tan, B., J. Hu, P. Zhang, D. Huang, N. V. Shabanov, M. Weiss, Y. Knyazikhin, and R. B. Myneni (2005), Validation of MODIS LAI product in croplands of Alpilles, France, *J. Geophys. Res.*, *110*, D01107, doi:10.1029/2004JD004860.

Tan, B., C. E. Woodcock, J. Hu, P. Zhang, M. Ozdogan, D. Huang, W. Yang, Y. Knyazikhin, and R. B. Myneni (2006), The impact of gridding artifacts on the local spatial properties of MODIS data: Implications for validation, compositing, and band-to-band registration across resolutions, *Remote Sens. Environ.*, *105*(2), 98–114.

Tarnavsky, E. V., S. Garrigues, and M. E. Brown (2008), Multiscale Geostatistical Analysis of AVHRR, SPOT-VGT, and MODIS NDVI products, *Remote Sens. Environ.*, *112*(2), 535–549.

Tian, Y., Y. Wang, Y. Zhang, Y. Knyazikhin, J. Bogaert, and R. B. Myneni (2002), Radiative transfer based scaling of LAI/FPAR retrievals from reflectance data of different resolutions, *Remote Sens. Environ.*, *84*, 143–159.

Tian, Y., et al. (2004), Comparison of seasonal and spatial variations of leaf area index and fraction of absorbed photosynthetically active radiation from Moderate Resolution Imaging Spectroradiometer (MODIS) and Common Land Model, *J. Geophys. Res.*, *109*, D01103, doi:10.1029/2003JD003777.

Turner, D. P., W. B. Cohen, R. E. Kennedy, K. S. Fassnacht, and J. M. Briggs (1999), Relationships between leaf area index, fapar and net primary production of terrestrial ecosystems, *Remote Sens. Environ.*, *70*, 52–68.

Verger, A., F. Baret, and M. Weiss (2008), Performances of neural networks for deriving LAI estimates from existing MODIS and CYCLOPES products, *Remote Sens. Environ.*, in press.

Verhoef, W. (1984), Light scattering by leaf layers with application to canopy reflectance modeling: The SAIL model, *Remote Sens. Environ.*, *16*, 125–141.

Vermote, E. F., D. Tanré, J. L. Deuzé, M. Herman, and J. J. Mocrette (1997), Second simulation of the satellite signal in the solar spectrum, 6S: An overview, *IEEE Trans. Geosci. Remote Sens.*, *35*(3), 675–686.

Wang, Y., Y. Tian, Y. Zhang, N. El-Saleous, Y. Knyazikhin, E. Vermote, and R. B. Myneni (2001), Investigation of product accuracy as a function of input and model uncertainties: Case study with SeaWiFS and MODIS LAI/FPAR algorithm, *Remote Sens. Environ.*, *78*, 296–311.

Wang, Y., et al. (2004), Evaluation of the MODIS LAI algorithm at a coniferous forest site in Finland, *Remote Sens. Environ.*, *91*, 114–127.

Weiss, M., and F. Baret (1999), Evaluation of canopy biophysical variable retrieval performances from the accumulation of large swath satellite data, *Remote Sens. Environ.*, *70*, 293–306.

Weiss, M., F. Baret, G. J. Smith, I. Jonckheere, and P. Coppin (2004), Review of methods for in situ leaf area index (LAI) determination: Part II. Estimation of LAI, errors and sampling, *Agric. For. Meteorol.*, *121*(1–2), 37–53.

Weiss, M., F. Baret, S. Garrigues, and R. Lacaze (2007), LAI and fAPAR CYCLOPES global products derived from VEGETATION. part 2: Validation and intercomparison with MODIS Collection 4 products, *Remote Sens. Environ.*, *110*(3), 317–331.

Xiao, X., S. Hagen, Q. Zhang, M. Keller, and B. Moore III (2006), Detecting leaf phenology of seasonally moist tropical forests in South America with multi-temporal MODIS images, *Remote Sens. Environ.*, *103*(4), 465–473.

Yang, W., D. Huang, B. Tan, J. C. Stroeve, N. V. Shabanov, Y. Knyazikhin, R. R. Nemani, and R. B. Myneni (2006a), Analysis of leaf area index and fraction vegetation absorbed PAR products from the Terra MODIS sensor: 2000–2005, *IEEE Trans. Geosci. Remote Sens.*, *44*(7), 1829–1842.

Yang, W., et al. (2006b), MODIS leaf area index products: From validation to algorithm improvement, *IEEE Trans. Geosci. Remote Sens.*, *44*(7), 1885–1898.

Yang, W., N. V. Shabanov, D. Huang, W. Wang, R. E. Dickinson, R. R. Nemani, Y. Knyazikhin, and R. B. Myneni (2006c), Analysis of leaf area index products from combination of MODIS Terra and Aqua data, *Remote Sens. Environ.*, *104*(3), 297–312.

Zhang, P., B. Anderson, M. Barlow, B. Tan, and R. B. Myneni (2004), Climate-related vegetation characteristics derived from Moderate Resolution Imaging Spectroradiometer (MODIS) leaf area index and normalized difference vegetation index, *J. Geophys. Res.*, *109*, D20105, doi:10.1029/2004JD004720.

Zhang, P., B. Anderson, B. Tan, D. Huang, and R. Myneni (2005), Potential monitoring of crop production using a satellite-based Climate-Variability Impact Index, *Agric. For. Meteorol.*, *132*(3–4), 344–358.

F. Baret and M. Weiss, INRA-EMMAH, UMR 1114, CEDEX 9, Avignon 84914, France.

R. Fernandes, Canada Centre for Remote Sensing, Ottawa, ON K1A 0Y7, Canada.

S. Garrigues, Earth System Science Interdisciplinary Center, University of Maryland, NASA Goddard Space Flight Center, Greenbelt, MD 20770, USA. (sebastien.garrigues@gsfc.nasa.gov)

Y. Knyazikhin, R. B. Myneni, N. V. Shabanov, and W. Yang, Department of Geography and Environment, Boston University, Boston, MA 02215, USA.

R. Lacaze, POSTEL Service Center/MEDIAS-France, CEDEX 9, Toulouse 31401, France.

J. T. Morisette, NASA Goddard Space Flight Center, Greenbelt, MD 20771, USA.

J. E. Nickeson, INOVIM, NASA Goddard Space Flight Center, Greenbelt, MD 20771, USA.

S. Plummer, IGBP-European Space Agency, Frascatti 00044, Italy.